



Originally published as:

Schuessler, J. A., Kämpf, H., Koch, U., Alawi, M. (2016): Earthquake impact on iron isotope signatures recorded in mineral spring water. - *Journal of Geophysical Research*, 121, 12, pp. 8548—8568.

DOI: <http://doi.org/10.1002/2016JB013408>

## RESEARCH ARTICLE

10.1002/2016JB013408

## Key Points:

- First Fe isotope time series study of mineral spring water over 3 years covering periods before, during, and after seismic activity
- Earthquakes change fluid/rock interaction and biogeochemical reactions in the aquifer, detected by hydrochemical and Fe isotope signatures
- Fe isotope signatures in spring water show recurring negative  $\delta^{56}\text{Fe}$  anomalies as low as  $-0.3$  after a time lag of a seismic swarm occurrence

## Supporting Information:

- Supporting Information S1–S3

## Correspondence to:

J. A. Schuessler,  
jan.schuessler@gfz-potsdam.de

## Citation:

Schuessler, J. A., H. Kämpf, U. Koch, and M. Alawi (2016), Earthquake impact on iron isotope signatures recorded in mineral spring water, *J. Geophys. Res. Solid Earth*, 121, 8548–8568, doi:10.1002/2016JB013408.

Received 28 JUL 2016

Accepted 1 DEC 2016

Accepted article online 6 DEC 2016

Published online 22 DEC 2016

## Earthquake impact on iron isotope signatures recorded in mineral spring water

Jan A. Schuessler<sup>1</sup> , Horst Kämpf<sup>2</sup>, Ulrich Koch<sup>3</sup>, and Mashal Alawi<sup>4</sup>

<sup>1</sup>GFZ German Research Centre for Geosciences, Earth Surface Geochemistry, Potsdam, Germany, <sup>2</sup>GFZ German Research Centre for Geosciences, Organic Geochemistry, Plauen, Germany, <sup>3</sup>Plauen, Germany, <sup>4</sup>GFZ German Research Centre for Geosciences, Geomicrobiology, Potsdam, Germany

**Abstract** We investigated the iron isotope signatures of dissolved Fe in the water of the Wettinquelle mineral spring (Bad Brambach, Germany) by time series sampling covering seismically active periods related to tectonic activity near the Eger Rift system in central Europe. Our objective was to test whether Fe isotopes trace earthquake-induced abiotic and biotic changes in the fluid/rock interaction of the deep, fissured, granitic aquifer. We found that the dissolved Fe isotope signatures in spring water are distinct from the granitic source signature ( $\delta^{56}\text{Fe} = +0.09\%$ ). Particularly, we discovered that water  $\delta^{56}\text{Fe}$  values are remarkably stable ( $-0.01 \pm 0.11\%$ , 2SD,  $n = 4$ ) before and during a strong seismic swarm period in 2000 (local magnitudes  $M_L > 3$ ), while  $\text{O}_2$  and  $\text{H}_2$  concentrations in water decrease and dissolved Fe content increases. Later, recurring events of lower  $\delta^{56}\text{Fe}$  values down to  $-0.3\%$  are observed in the period from 2001 to 2003 with intermittent seismic events ( $1 < M_L < 3.2$ ). The observations indicate a time lag between tectonic forcing and Fe isotope response. The role of abiotic fluid/rock interaction and Fe-utilizing bacteria identified in the mineral spring water on Fe isotope fractionation is discussed. We explain recurring changes toward isotopically lighter values by a combination of Fe dissolution from deep granite and admixture of isotopically light Fe generated by a complex combination of abiotic and biotic processes operating in the aquifer when disturbed by swarm earthquakes events. We propose a conceptual model scenario of earthquake-triggered changes in biogeochemical processes.

### 1. Introduction

Studies on earthquake-related impact on fluid compositions using element concentrations or isotope ratios highlight the potential of geochemical signals to decipher seismically induced changes in fluid-rock interactions. Previous studies found strong changes in dissolved element concentrations prior, during, or after an earthquake. For example, chloride concentration and lead isotope anomalies were found in spring water starting a few days prior to the 1996 earthquake (magnitude  $M_L = 5.2$ ) in the Pyrenean [Poitrasson *et al.*, 1999; Toutain *et al.*, 2006] and the major  $M = 7.2$  Kobe earthquake in 1995 [Tsunogai and Wakita, 1995], respectively, and were attributed to preseismic strain change inducing mixing of different aquifers. Such earthquake-related hydrochemical signals were also observed in other tectonically active regions. Several anomalies in hydrogen and oxygen stable isotope ratios occurred immediately after seismic events near Acapulco, Mexico [Taran *et al.*, 2005], and related to a  $M = 5.1$  earthquake in 2005 at Koyna, India [Reddy *et al.*, 2011], respectively. Similarly, a transient geochemical groundwater anomaly occurred after the 1998 Adana earthquake in Turkey [Woith *et al.*, 2013]. Moreover, swarm earthquakes triggered isotopic anomalies that were identified by time series analyses of dissolved gases in spring water in the Western Eger Rift area, central Europe [e.g., Kämpf *et al.*, 1989; Bräuer *et al.*, 2007]. More recently, chemical and isotopic time series analysis of groundwater samples were obtained over several years combined with detailed petrological studies on drill cores related to consecutive  $M > 5$  earthquakes in northern Iceland [e.g., Skelton *et al.*, 2014; Wasteby *et al.*, 2014; Andrén *et al.*, 2016]. There, dissolved element concentrations, as well as oxygen and hydrogen stable isotope ratios observed in groundwater, showed pre-earthquake anomalies, and their subsequent decay was related to mixing of different groundwater components variably affected by water rock interaction, nonstoichiometric mineral dissolution, and mineralogical alteration reactions in the fractured rock aquifer, respectively. These processes were explained by expansion of the rock volume (dilation), therefore enhancing permeability. Generally, previous studies highlight the specific behavior of different elements and their isotopes in aquifers affected by earthquakes. Their dependence on lithology and other environmental conditions offers the opportunity to study different biogeochemical processes affected by seismic

activity. Moreover, the activity of the deep subsurface biosphere is increasingly explored, revealing the significance of this habitat for biogeochemical cycles and evidence for deep biosphere activity related to earthquakes [Bräuer *et al.*, 2005; Kietavainen and Purkamo, 2015; Lin *et al.*, 2006; Pedersen, 2000, 2012; Schreiber *et al.*, 2012; Sherwood Lollar *et al.*, 2014; Sherwood Lollar *et al.*, 2007].

Particularly, iron plays an important role in the abiotic and biotic reactions in the subsurface, and therefore, Fe isotope measurements in groundwater offer the potential to reveal insights into earthquake-triggered changes in fluid-solid interactions. However, the potential impact of earthquakes on Fe isotope signatures in deep aquifers—and the associated spring water emanating at the surface—has not been investigated to date. The objective of this study is to test whether Fe isotopes in mineral spring water trace earthquake-induced changes in fluid-rock interaction and in biogeochemical cycles that are active in a fissured granitic aquifer. For this study we made use of a unique “natural laboratory” setting, where long-term geophysical and geochemical monitoring was established.

Fe isotopes are a tool to investigate the physical and chemical reactions in which Fe is involved (and their seismically induced changes) as Fe is moving from depth toward the surface, emerging as dissolved Fe in spring water. Iron isotope fractionation occurs due to changes in Fe redox state, abiotic and biotic reactions, such as microbial utilization, or hydrothermal and low-temperature secondary mineral formation (see review by Wiederhold [2015]). Biogeochemical reactions that involve Fe transfer between different compounds control the Fe isotopic composition of water, rock, and plants, for example. In particular, redox reactions that involve ferric ( $\text{Fe}^{3+}$ ) and ferrous ( $\text{Fe}^{2+}$ ) iron can produce specific iron isotope fingerprints, making the Fe isotope system a valuable tool to trace biogeochemical processes. The equilibrium isotope fractionation between aqueous Fe(II) and Fe(III) is one of the best studied systems, both from experimental and theoretical investigations [Anbar *et al.*, 2005; Johnson *et al.*, 2002; Welch *et al.*, 2003], exhibiting a large fractionation of about 3‰ in the  $^{56}\text{Fe}/^{54}\text{Fe}$  ratio. In aqueous solutions, Fe is mobile in its ferrous form under anoxic conditions of low or neutral pH, while ferric Fe is only soluble in acidic solutions and, in oxic environments, it readily forms precipitates, such as amorphous and crystalline oxides, which are isotopically fractionated compared to dissolved Fe [Skulan *et al.*, 2002; Welch *et al.*, 2003; Wiesli *et al.*, 2004]. Organic matter, mineral surfaces, and colloids interact with Fe mainly by sorption processes and contribute to its mobility in systems containing aqueous solutions. Experimental studies have shown Fe isotope fractionation associated with these processes. In particular, mineral dissolution [e.g., Brantley *et al.*, 2004; Chapman *et al.*, 2009], Fe complexation by organic ligands [e.g., Morgan *et al.*, 2010], and sorption onto clay minerals [e.g., Beard *et al.*, 2010; Mikutta *et al.*, 2009] cause heavy isotope enrichments in the solid phases (i.e., remaining minerals, organic complexes, and adsorbed), leaving an isotopically light solution. Experimental studies on biologically mediated Fe isotope fractionation [e.g., Brantley *et al.*, 2004; Croal *et al.*, 2004; Crosby *et al.*, 2007; Kappler *et al.*, 2010] highlight the importance of biological activity in the interpretation of isotopic signatures in environments suitable for living organisms. To date, only few data of Fe isotope compositions of deep groundwater exist [Guo *et al.*, 2013; Teutsch *et al.*, 2005; Xie *et al.*, 2014]. These studies showed that Fe isotopes are strongly controlled by redox processes in the aquifer.

The NW Bohemia/Vogtland region is a nonvolcanic region in which active geodynamic processes (earthquake swarms) have been the subject of detailed, long lasting, time series sampling for geochemical, microbiological, and geophysical studies [Wagner *et al.*, 2007; Bräuer *et al.*, 2014, and references therein]. This region provides an ideal natural laboratory to study earthquake-triggered changes in biogeochemical processes. The continuous water sample monitoring over seismically active and quiet periods at the Wettingquelle spring opens a unique opportunity to study whether Fe isotopes provide a characteristic fingerprint of the processes described above. Do seismically induced changes in abiotic or biotic reactions in the deep fissured granitic aquifer occur and, if so, are they reflected by the Fe isotope signatures of the water emerging at the surface? Here we investigate the Fe isotope signatures of dissolved Fe and the concentration of other dissolved elements in the Wettingquelle mineral spring water over more than 3 years (May 2000 to December 2003), covering several seismic events, where the largest swarm period ( $M_L = 3.2$ ) started on 28 August 2000 and lasted until the end of January 2001 [Horálek and Šílený, 2013]. Our analyses show that the hydrochemical compositions and Fe isotope ratios of dissolved Fe are affected by recurring seismic events. We discuss the microbial impact as well as inorganic processes controlled by water-rock interaction in the deep fractured granite and the shallow oxygenated aquifer, traced by Fe isotopes. Finally, we propose a conceptual model describing the tectonic forcing on biogeochemical processes and isotopic fractionation.

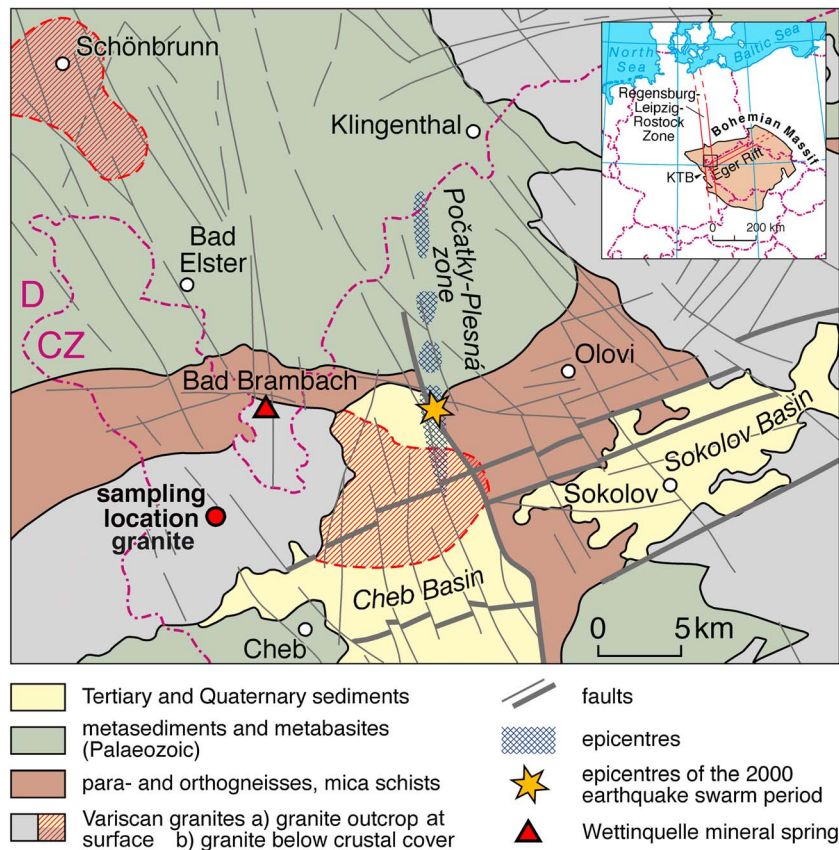


**Figure 1.** Location of the spring water sampling site at the Wettingquelle mineral spring (red triangle) in Bad Brambach, Germany (D), close to the border to the Czech Republic (CZ). Also shown are geological units, major faults, and seismic epicenter locations for the strong 2000 earthquake swarm event (star) and other seismic events in this area (modified from *Baumann et al.* [1982] and *Weise et al.* [2001]). The red circle indicates the sampling location of the granite bedrock sample.

## 2. Field Site and Methods

### 2.1. Study Site

The southern Vogtland/Germany and NW Bohemia/Czech Republic region (Figure 1) has been host to the most intense earthquake swarms in central Europe. The seismic energy of this type of seismicity is released through a sequence of numerous small- to medium-sized events at shallow focal depths, with no distinct main shock. Reoccurring earthquake activity has been well documented since the nineteenth century in the northwestern part of the Bohemian massif [*Credner*, 1876; *Knett*, 1899]. The present seismic activity is concentrated at the intersection of the Eger Rift (ER) and the Regensburg-Leipzig-Rostock Zone (RLRZ), where the Tertiary Cheb Basin was formed (Figure 1, map inset) as a result of the reactivation of Hercynian faults and/or separated microplates (Saxothuringian, Moldanubian, and Tepla-Barrandean unit) during the Late Tertiary and Quaternary [*Babuska and Plomerova*, 2008; *Bankwitz et al.*, 2003]. The focal depths of the intra-plate seismic swarms of the whole area with maximum magnitudes of up to 4.5 are located between 4 and 20 km [*Horálek and Fischer*, 2010]. Most of the earthquake activity is concentrated at the Nový Kostel focal zone (NKFZ), located at the intersection between the N-S trending Počátky-Plesná Fault Zone (PPZ) and the NW trending Mariánské Lázně Fault Zone (Figure 1). The area is characterized by increased heat flow, Quaternary volcanism active until the middle Pleistocene [*Mrlina et al.*, 2009], hydrothermal activity from the middle Pleistocene to the Holocene [*Vylita et al.*, 2007], seismic activity along faults related to the N-S trending RLRZ seismoactive zone [*Bankwitz et al.*, 2003; *Peterek et al.*, 2011; *Fischer et al.*, 2014; *Horálek and Fischer*, 2010; *Neunhöfer and Hemmann*, 2005], and juvenile CO<sub>2</sub>-rich springs associated with isotopic anomalies of mantle-derived He [*Bräuer et al.*, 2005; *Bräuer et al.*, 2011; *Bräuer et al.*, 2008; *Kämpf et al.*, 2013; *Nickschick et al.*, 2015; *Weinlich et al.*, 1999]. The 2000 swarm was of a distinctly episodic character: most of the events occurred during nine swarm phases lasting from 2 to 4 days and were separated by quiescence

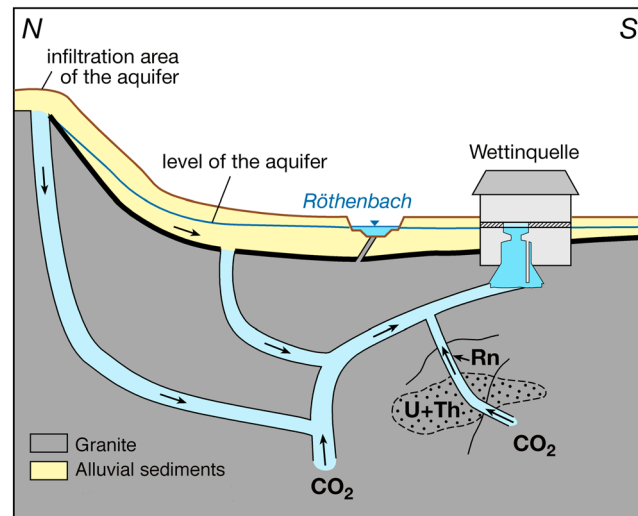


**Figure 2.** Schematic representation of the Wettingquelle aquifer (not to scale, simplified illustration after Koch *et al.* [2005]). The deep granite aquifer is characterized by fractures related to tectonic activity, which allow fluid transport (mineralized water and gases) from depth toward the surface, where they mix with 10 to 20% of young surface water that infiltrates through sediments (alluvial deposits and clay-bearing sand/gravel) and fractured granite, eventually emanating at the Wettingquelle spring capture. Between the sediments and the granite a transition zone of weathered granite exists.

a few of them have been studied in detail [e.g., Kämpf *et al.*, 2013]. The Wettingquelle mineral spring in Bad Brambach, Germany, is located 10 km west of the NKFZ (Figure 1). The dominating rocks include sequences from Upper Cambrian to Ordovician age and areas with Late Variscan intrusions dominated by granites. The deep aquifer of the Wettingquelle mineral spring is situated in the fissured Fichtelgebirge/Smrčiny granite [Hecht *et al.*, 1997]. The water reaches the surface along fractures and faults (Figure 2) [Koch *et al.*, 2005]. Previous studies reported on the gas composition and methane  $\delta^{13}\text{C}$  values from a weekly sampling campaign at the Wettingquelle mineral spring between 2000 and 2003 covering the more than 3 month long earthquake swarm period in 2000. Seismically induced changes of fluid composition were impressively demonstrated by the temporal variation of methane concentration in the Wettingquelle gas and carbon isotopic values of methane [Bräuer *et al.*, 2005; Bräuer *et al.*, 2007]. The spring water contains high concentrations of dissolved elements, such as sodium, calcium, iron, bicarbonate, and sulfate combined with a remarkably high radon activity of 27 kBq/L water [Bräuer *et al.*, 2007; Koch and Heinicke, 2011]. Bräuer *et al.* [2005, 2007] observed a rise in the methane concentration starting about 8 weeks after the beginning of the swarm earthquake period in 2000 from about 40 up to 250 ppmv, which was accompanied by decreasing  $\delta^{13}\text{C}_{\text{CH}_4}$  values from around  $-50$  to  $-70\text{‰}$ . This shift of the  $\delta^{13}\text{C}_{\text{CH}_4}$  values indicates a microbial origin of the additionally formed methane, which is most likely produced by methanogens in the deep fissured granite where the Wettingquelle is captured, using stress-released  $\text{H}_2$  as energy source [Bräuer *et al.*, 2005, 2008]. The authors suggested that the delayed arrival of the seismically induced microbial methane was attributed to the transport time of the methane from the area of formation (deep granite) to the subsurface. The bacterial communities found in the deep aquifer of the Wettingquelle water sampled 1 year after the earthquake swarm in 2000 contain close relatives of *Gallionella ferruginea*, a microaerobic oxidizer of ferrous iron and other Fe-utilizing bacteria [Wagner *et al.*, 2007].

## 2.2. Sampling and Analytical Methods

Water samples from time series sampling at the Wettingquelle mineral spring (50.2207°N, 12.3038°E, Figure 1) were analyzed covering more than 3 years—from May 2000 to December 2003. Sampling was carried out weekly for the first 2 years and fortnightly in the last year during the course of previous monitoring studies [Bräuer *et al.*, 2007]. The oxygen concentration in water was measured at the spring capture (Multi 3420

periods. The seismic activity culminated during the eighth phase (5–7 November), in which four  $M_L \geq 3$  earthquakes occurred [Fischer, 2003; Horálek and Šílený, 2013]. The swarm was located in the southern part of the main Nový Kostel focal zone, where the fault plane is striking 168°N and dipping 80° westward, Figure 1 [Fischer and Horálek, 2005]. Previous studies suggested a connection between the common occurrence of deep-seated fluids (mostly mantle-derived  $\text{CO}_2$ -rich fluids) and seismicity, where the observed anomalies may reflect a seismically induced release of fluids and/or changes in fluid migration pathways [Bachura and Fischer, 2016; Bräuer *et al.*, 2011; Bräuer *et al.*, 2008; Faber *et al.*, 2009; Horálek and Fischer, 2008; Koch *et al.*, 2008; Koch and Heinicke, 2011; Kämpf *et al.*, 1989].

More than 100 mineral springs and several hundred gas vents emerge at the intersections of the fault zones, but only

**Table 1.** Analytical Results of Water Samples<sup>a</sup>

Sampling Date (Day/Month/Year)	K (mg/L)	Na (mg/L)	Ca (mg/L)	Mg (mg/L)	Si (mg/L)	Fe (mg/L)	S (mg/L)	Mn (mg/L)	Sr (mg/L)	Li (mg/L)	Al (mg/L)	$\delta^{56}\text{Fe}$ (‰)	$\delta^{57}\text{Fe}$ (‰)	O <sub>2</sub> Measurement Date (Day/Month/Year)	O <sub>2</sub> in Water (mg/L)
<i>Mineral Spring Water (Wettersquelle, Bad Brambach, Germany)</i>															
02/05/2000	9.7	214	176	28	25	8.0	82	0.69	0.68	0.57		0.00	-0.03	26/07/2000	0.39
31/05/2000	9.6	211	172	28	25	8.8	82	0.72	0.71	0.57	0.30			01/08/2000	0.37
07/06/2000	10.0	211	173	28	25	8.3	81	0.71	0.70	0.56	0.30			25/08/2000	0.28
28/06/2000	9.6	218	171	27	25	8.7	82	0.70	0.67	0.58		0.06	0.10	30/08/2000	0.33
04/07/2000	10.2	222	176	28	26	9.2	84	0.74	0.72	0.59	0.30			06/09/2000	0.26
12/07/2000	9.6	212	168	27	25	8.8	81	0.73	0.69	0.56	0.29			13/09/2000	0.25
19/07/2000	9.9	219	173	29	26	9.1	84	0.74	0.71	0.58	0.30			20/09/2000	0.23
26/07/2000	9.7	213	165	27	25	8.7	81	0.70	0.68	0.57	0.28			27/09/2000	0.27
25/08/2000	10.5	226	170	27	26	9.4	84	0.72	0.69	0.60	0.29			04/10/2000	0.24
30/08/2000	9.7	220	163	27	25	9.4	83	0.70	0.67	0.59	0.29			12/10/2000	0.04
06/09/2000	10.6	229	173	28	26	9.7	86	0.74	0.71	0.61	0.30			25/10/2000	0.11
13/09/2000	10.1	224	169	28	26	9.7	85	0.74	0.70	0.60	0.29			01/11/2000	0.05
20/09/2000	10.2	232	171	28	26	9.9	86	0.72	0.67	0.62		-0.05	-0.08	07/11/2000	0.10
27/09/2000	9.7	216	164	27	25	9.7	82	0.71	0.67	0.58	0.29			15/11/2000	0.02
04/10/2000	10.3	219	165	27	25	9.6	82	0.71	0.68	0.58	0.28			21/11/2000	0.05
12/10/2000	9.8	215	163	27	25	9.9	82	0.71	0.67	0.58	0.28			28/11/2000	0.04
25/10/2000	10.1	219	163	27	25	10.1	82	0.69	0.66	0.59	0.29			06/12/2000	0.05
01/11/2000	10.1	230	169	29	27	10.8	88	0.73	0.70	0.62	0.28			13/12/2000	0.07
07/11/2000	10.4	224	162	27	25	10.3	83	0.69	0.66	0.60	0.28			20/12/2000	0.06
15/11/2000	9.8	224	162	27	26	10.6	84	0.71	0.67	0.60	0.28			05/01/2001	0.10
21/11/2000	10.0	233	165	28	25	10.8	85	0.69	0.65	0.62		-0.05	-0.04	10/01/2001	0.02
28/11/2000	9.8	220	162	27	25	10.8	83	0.71	0.66	0.59	0.27			17/01/2001	0.04
06/12/2000	10.5	228	169	28	26	11.1	86	0.73	0.69	0.61	0.29			24/01/2001	0.07
20/12/2000	9.8	220	165	28	26	11.2	83	0.72	0.68	0.59	0.28			31/01/2001	0.05
05/01/2001	10.2	222	160	27	25	10.8	82	0.67	0.65	0.59	0.26			08/02/2001	0.11
10/01/2001	9.8	219	167	28	26	11.3	83	0.73	0.68	0.58	0.26			14/02/2001	0.10
17/01/2001	10.1	225	167	28	26	11.6	84	0.71	0.68	0.60	0.27			21/02/2001	0.04
24/01/2001	9.6	224	160	27	25	11.0	82	0.66	0.62	0.60		-0.01	0.00	01/03/2001	0.07
31/01/2001	9.9	225	164	28	26	11.5	84	0.71	0.67	0.60	0.26			07/03/2001	0.11
14/02/2001	9.3	204	162	27	25	10.4	79	0.69	0.67	0.55	0.26			14/03/2001	0.07
21/02/2001	9.8	219	167	28	26	11.2	84	0.72	0.69	0.59	0.29			21/03/2001	0.11
01/03/2001	9.7	228	168	28	25	11.1	85	0.69	0.65	0.62		-0.02	0.02	04/04/2001	0.12
07/03/2001	9.8	219	165	27	25	11.0	82	0.70	0.67	0.59	0.27			11/04/2001	0.10
14/03/2001	9.4	203	167	27	25	10.4	79	0.72	0.69	0.55	0.27	-0.17	-0.26	18/04/2001	0.04
21/03/2001	9.4	204	164	27	25	9.9	79	0.67	0.67	0.55	0.27			25/04/2001	0.05
04/04/2001	9.0	204	160	26	24	9.1	76	0.62	0.62	0.55		-0.07	-0.10	02/05/2001	0.04
11/04/2001	9.2	202	160	26	25	9.6	78	0.65	0.65	0.55	0.28			08/05/2001	0.07
18/04/2001	9.2	200	158	26	24	9.5	76	0.64	0.65	0.54	0.27			16/05/2001	0.10
25/04/2001	9.0	200	158	26	24	9.4	77	0.65	0.65	0.54	0.27			23/05/2001	0.05
02/05/2001	8.9	198	156	25	24	9.1	76	0.64	0.64	0.53	0.27			30/05/2001	0.11
08/05/2001	9.0	203	158	26	24	9.3	76	0.65	0.65	0.54	0.27			07/06/2001	0.11
16/05/2001	9.5	210	161	26	25	9.5	79	0.65	0.66	0.56	0.28			12/06/2001	0.13
23/05/2001	9.5	217	166	27	26	10.0	82	0.68	0.68	0.58	0.28			20/06/2001	0.13
30/05/2001	9.4	221	163	27	25	9.5	81	0.64	0.63	0.59		-0.06	-0.07	27/06/2001	0.11
07/06/2001	9.3	210	163	27	25	9.5	80	0.67	0.67	0.56	0.26			20/07/2001	0.10
12/06/2001	9.4	212	165	27	25	9.6	80	0.67	0.68	0.57	0.27			25/07/2001	0.11
20/06/2001	9.5	215	169	27	26	9.7	81	0.69	0.70	0.57	0.27			01/08/2001	0.10
27/06/2001	9.1	205	163	26	25	9.2	78	0.66	0.67	0.55	0.27			28/08/2001	0.11
20/07/2001	9.1	202	160	25	24	8.7	76	0.63	0.66	0.53	0.26			04/09/2001	0.17
25/07/2001	9.2	205	161	26	25	9.1	78	0.65	0.67	0.54	0.27			12/09/2001	0.10
01/08/2001	9.4	215	160	27	25	9.3	80	0.65	0.66	0.57	0.27			19/09/2001	0.11
08/08/2001	9.6	221	161	27	25	9.4	82	0.65	0.67	0.59	0.28			26/09/2001	0.10
15/08/2001	9.6	224	161	27	26	9.7	83	0.65	0.66	0.60	0.28			04/10/2001	0.13
22/08/2001	9.8	232	163	27	25	9.4	84	0.64	0.64	0.62		0.02	0.09	10/10/2001	0.07
28/08/2001	10.0	232	163	27	26	9.8	85	0.66	0.67	0.62	0.29	-0.13	-0.22	17/10/2001	0.10
04/09/2001	10.4	236	166	28	27	9.8	87	0.66	0.68	0.63	0.28			24/10/2001	0.10
12/09/2001	9.9	221	157	26	25	9.1	81	0.63	0.65	0.59	0.27			30/10/2001	0.07

**Table 1.** (continued)

Sampling Date (Day/Month/Year)	K (mg/L)	Na (mg/L)	Ca (mg/L)	Mg (mg/L)	Si (mg/L)	Fe (mg/L)	S (mg/L)	Mn (mg/L)	Sr (mg/L)	Li (mg/L)	Al (mg/L)	$\delta^{56}\text{Fe}$ (‰)	$\delta^{57}\text{Fe}$ (‰)	O <sub>2</sub> Measurement Date (Day/Month/Year)	O <sub>2</sub> in Water (mg/L)
19/09/2001	9.6	219	160	27	25	9.2	82	0.65	0.66	0.59	0.27			07/11/2001	0.12
26/09/2001	9.4	212	157	26	25	9.0	79	0.63	0.65	0.56	0.26			14/11/2001	0.09
04/10/2001	9.6	214	157	26	25	8.9	79	0.62	0.65	0.57	0.25			20/11/2001	0.17
10/10/2001	9.6	213	161	27	25	9.0	80	0.64	0.67	0.57	0.26			27/11/2001	0.11
17/10/2001	10.2	228	169	28	27	9.5	86	0.67	0.70	0.61	0.28			04/12/2001	0.04
24/10/2001	10.4	234	170	28	27	9.6	88	0.67	0.70	0.63	0.28			12/12/2001	0.20
30/10/2001	9.8	228	163	27	25	8.9	84	0.62	0.64	0.62		-0.03	-0.05	19/12/2001	0.04
07/11/2001	10.0	229	163	28	26	9.3	85	0.65	0.68	0.61	0.28			04/01/2002	0.14
14/11/2001	9.6	209	160	26	25	8.8	79	0.63	0.66	0.56	0.26			16/01/2002	0.18
20/11/2001	9.6	213	160	27	25	8.9	80	0.63	0.66	0.57	0.26			23/01/2002	0.17
27/11/2001	9.6	217	160	27	25	8.9	81	0.63	0.66	0.58	0.26			30/01/2002	0.19
04/12/2001	9.2	196	156	25	24	8.3	75	0.60	0.65	0.53	0.26			06/02/2002	0.11
12/12/2001	9.6	203	163	27	26	8.8	78	0.63	0.68	0.55	0.27			12/02/2002	0.18
19/12/2001	9.5	202	158	26	24	8.3	76	0.61	0.65	0.54	0.26			20/02/2002	0.16
04/01/2002	9.4	216	161	26	25	8.3	79	0.61	0.64	0.58		-0.02	0.00	27/02/2002	0.11
16/01/2002	9.6	215	161	27	25	8.6	80	0.63	0.67	0.57	0.27			06/03/2002	0.11
23/01/2002	9.3	204	159	26	24	8.1	77	0.63	0.66	0.54	0.27			13/03/2002	0.17
30/01/2002	8.7	185	149	24	24	7.9	71	0.56	0.61	0.49	0.24			20/03/2002	0.16
06/02/2002	8.9	194	154	25	24	7.7	74	0.58	0.64	0.52	0.26			26/03/2002	0.19
12/02/2002	9.1	199	156	26	24	7.8	76	0.60	0.65	0.53	0.26			04/04/2002	0.10
20/02/2002	8.9	191	155	25	24	7.9	72	0.58	0.64	0.51	0.28	-0.17	-0.25	10/04/2002	0.17
27/02/2002	8.8	191	153	25	24	8.1	72	0.57	0.63	0.51	0.27			17/04/2002	0.19
06/03/2002	8.7	188	151	25	24	7.8	72	0.56	0.62	0.50	0.27			30/04/2002	0.10
13/03/2002	8.9	194	152	25	24	7.8	73	0.57	0.62	0.52	0.28			08/05/2002	0.12
20/03/2002	8.4	193	147	25	24	7.7	73	0.56	0.60	0.52	0.27			22/05/2002	0.11
26/03/2002	8.4	183	146	24	23	7.5	70	0.54	0.60	0.50	0.26			05/06/2002	0.14
04/04/2002	8.7	198	152	25	24	7.5	73	0.54	0.60	0.53		-0.11	-0.15	18/06/2002	0.15
10/04/2002	8.5	194	148	25	24	7.6	74	0.56	0.61	0.52	0.28			02/07/2002	0.09
17/04/2002	8.7	201	152	26	24	7.7	76	0.58	0.62	0.54	0.27			17/07/2002	0.20
30/04/2002	8.9	201	154	26	24	7.6	76	0.57	0.63	0.54	0.26			31/07/2002	0.28
08/05/2002	8.9	208	155	26	24	7.7	78	0.59	0.64	0.55	0.27			14/08/2002	0.28
22/05/2002	8.8	205	155	26	24	7.7	77	0.58	0.64	0.54	0.27			18/09/2002	0.28
05/06/2002	8.9	208	156	26	24	7.8	78	0.58	0.64	0.55	0.26			01/10/2002	0.31
18/06/2002	8.8	200	157	26	24	7.8	76	0.58	0.64	0.53	0.26			15/10/2002	0.26
02/07/2002	9.1	214	156	26	25	7.8	79	0.59	0.65	0.56	0.26			29/10/2002	0.26
17/07/2002	9.2	215	153	26	25	7.9	80	0.58	0.63	0.57	0.27			12/11/2002	0.28
31/07/2002	9.2	218	153	26	25	7.9	81	0.58	0.63	0.58	0.26	-0.24	-0.34	27/11/2002	0.25
14/08/2002	8.9	201	153	25	24	8.1	76	0.57	0.63	0.53	0.24			11/12/2002	0.32
18/09/2002	9.1	205	155	26	24	7.7	77	0.58	0.65	0.54	0.25			08/01/2003	0.29
01/10/2002	9.2	208	154	26	25	7.7	78	0.57	0.64	0.56	0.25			22/01/2003	0.29
15/10/2002	9.1	206	151	25	25	7.6	77	0.57	0.63	0.55	0.24			05/02/2003	0.27
29/10/2002	8.9	193	151	25	24	7.7	73	0.56	0.63	0.52	0.24			19/02/2003	0.29
12/11/2002	9.1	190	151	25	24	7.6	73	0.56	0.63	0.51	0.24			05/03/2003	0.31
27/11/2002	8.7	187	150	25	24	7.4	72	0.55	0.62	0.50	0.24			19/03/2003	0.24
08/01/2003	8.6	184	147	24	24	7.5	70	0.52	0.60	0.50	0.25	-0.05	-0.08	02/04/2003	0.32
22/01/2003	8.8	198	148	25	25	7.5	75	0.54	0.61	0.53	0.26			16/04/2003	0.35
05/02/2003	8.7	196	148	25	24	7.3	74	0.54	0.61	0.53	0.27			29/04/2003	0.32
19/02/2003	8.9	206	153	26	25	7.5	78	0.55	0.62	0.55	0.29			14/05/2003	0.36
05/03/2003	8.8	206	150	26	25	7.2	77	0.54	0.61	0.55	0.27			27/05/2003	0.37
19/03/2003	8.6	191	150	25	24	7.6	72	0.54	0.61	0.52	0.27			18/06/2003	0.27
02/04/2003	8.9	202	153	26	25	7.4	76	0.55	0.62	0.54	0.28			23/07/2003	0.29
29/04/2003	9.2	215	159	26	24	7.5	78	0.55	0.61	0.56		-0.09	-0.10	20/08/2003	0.33
14/05/2003	8.9	208	153	26	25	7.5	78	0.55	0.62	0.56	0.27	-0.30	-0.46	17/09/2003	0.28
27/05/2003	9.0	212	154	26	25	7.8	79	0.56	0.63	0.56	0.27				
18/06/2003	9.3	218	154	26	25	7.7	81	0.56	0.63	0.58	0.27				
23/07/2003	9.2	226	148	26	25	7.7	83	0.55	0.61	0.60	0.26				
20/08/2003	9.7	235	147	26	25	7.8	85	0.54	0.61	0.62	0.26	-0.26	-0.40		
17/09/2003	9.6	237	148	26	25	7.9	87	0.55	0.61	0.63	0.25				

Table 1. (continued)

Sampling Date (Day/Month/Year)	K (mg/L)	Na (mg/L)	Ca (mg/L)	Mg (mg/L)	Si (mg/L)	Fe (mg/L)	S (mg/L)	Mn (mg/L)	Sr (mg/L)	Li (mg/L)	Al (mg/L)	$\delta^{56}\text{Fe}$ (‰)	$\delta^{57}\text{Fe}$ (‰)	O <sub>2</sub> Measurement Date (Day/Month/Year)	O <sub>2</sub> in Water (mg/L)
15/10/2003	9.5	235	147	26	25	7.8	86	0.54	0.61	0.62	0.26				
12/11/2003	9.7	241	147	26	26	8.0	88	0.54	0.61	0.64	0.26				
09/12/2003	9.7	242	146	26	25	8.3	88	0.53	0.60	0.64	0.25				
<i>Surface/Stream Water From Bad Brambach, Germany (Röthenbach P01 to P05; Outcrop Spring P12)</i>															
15/05/2003 P01	1.5	7.7	11.7	2.9	7.0	0.26	12.6	0.065	0.065	<0.01	0.165	0.15	0.24		
15/05/2003 P02	1.3	7.1	10.6	2.5	6.9	0.20	11.3	0.050	0.057	<0.01	0.117	0.12	0.17		
15/05/2003 P03	2.4	9.8	15.5	5.1	8.0	0.04	13.4	0.011	0.098	<0.01	0.023				
15/05/2003 P04	1.4	7.4	10.7	2.6	6.9	0.17	11.3	0.049	0.058	<0.01	0.102				
15/05/2003 P05	1.5	8.5	12.5	3.1	7.2	0.29	11.8	0.071	0.068	<0.01	0.093				
15/05/2003 P12	2.3	7.4	12.8	3.0	8.0	<0.02	14.9	<0.01	0.064	<0.01	<0.02	0.13	0.20		

<sup>a</sup>Uncertainties are close to 5% relative for concentration data and were estimated based on reference materials measurements taking repeatability (2SD) and comparison of results to published reference values in to account. For Fe isotope data uncertainties are 0.05‰ (2SD) and 0.07‰ (2SD) for  $\delta^{56}\text{Fe}$  and  $\delta^{57}\text{Fe}$ , respectively. See supporting information Text S1 for analytical details.

digital analyzer, sensor FDO 925, WTW GmbH Weilheim) with a relative uncertainty of  $\pm 1.5\%$ . Water samples were filtered ( $<0.2\ \mu\text{m}$ ) and acidified to  $\text{pH} < 2$  with  $\text{HNO}_3$  for storage in PP bottles at  $4^\circ\text{C}$ . In addition, surface water samples from a nearby creek (Röthenbach, Figure 2) were analyzed. The chemical composition of the samples was analyzed by inductively coupled plasma optical emission spectroscopy (ICP-OES) with relative analytical uncertainties close to 5% (2 standard deviation, 2SD, i.e., representing 95% of the population), verified by analyses of reference materials and comparison to certified values and published data; SLRS-5 [Yeghicheyan *et al.*, 2013], NIST SRM 1640a, USGS M212, USGS T187, USGS T213, GFZ RW-1. The chemical composition of a granite bedrock sample (Figure 1) and a biotite mineral separate from this granite was also analyzed (X-ray fluorescence (XRF) and ICP-OES after alkali fusion and acid digestion, respectively) with relative analytical uncertainties (2SD) better than 10%, verified by analyses of reference materials (AC-E granite, BHVO-1, BHVO-2, BCR-2 basalts) [Dulski, 2001; Govindaraju, 1995; Jochum *et al.*, 2016]. Analytical procedures for concentration measurements are based on established procedures for sample preparation [Chao and Sanzolone, 1992; Potts, 1987; Riley, 1958; Totland *et al.*, 1992] and ICP-OES analyses [Ardini *et al.*, 2010; Baedecker, 1987; Dennaud *et al.*, 2001; Li, 1996; Marcos *et al.*, 2001; Walsh, 1992]. Our analytical protocol is described in detail in the supporting information Text S1.

Selected water samples from the Wettingquelle covering the seismically quiet and active periods, as well as the rock and minerals samples, were analyzed for their Fe isotope composition by multicollector inductively coupled plasma mass spectrometry (MC-ICP-MS) using the analytical protocol described in Schoenberg and von Blanckenburg [2005]. Uncertainties of this method are  $\pm 0.05\%$  and  $\pm 0.07\%$  (2SD) for  $\delta^{56}\text{Fe}$  and  $\delta^{57}\text{Fe}$ , respectively, which were verified during this study by analyses of reference materials and comparison to published data [Jochum *et al.*, 2005; Moeller *et al.*, 2014]. We discuss Fe isotope data in terms of  $\delta^{56}\text{Fe}$ , which is the per mil deviation of the  $^{56}\text{Fe}/^{54}\text{Fe}_{\text{sample}}$  ratio relative to the international isotope measurement standard IRMM-014. Further details on the analytical procedures are given in the supporting information Text S1.

### 3. Results

In general, element concentrations in the spring water vary significantly over time (Table 1 and Figure 3). Fe shows the most pronounced change during the strong earthquake swarm period around October 2000 and its preparatory phase of stress accumulation [Koch and Heinicke, 2011]. At this time also the measured O<sub>2</sub> concentration in spring water starts to decrease, while Fe concentration increases (Figures 5b and 5i). Moreover, spring discharge varies considerably over time (Figures 4 and 5d, discharge data from Bräuer *et al.* [2007]). Interestingly, the temporal pattern of amplitude changes in elemental signals is different when element mass fluxes in the spring water are considered (by multiplying the discharge with concentrations, Figure 3). The general pattern of elemental mass flux over time is mirrored by all elements (Figure 3), although Fe shows the strongest response in concentration to earthquake swarms. Some concentration data (e.g., Na, K, Si,



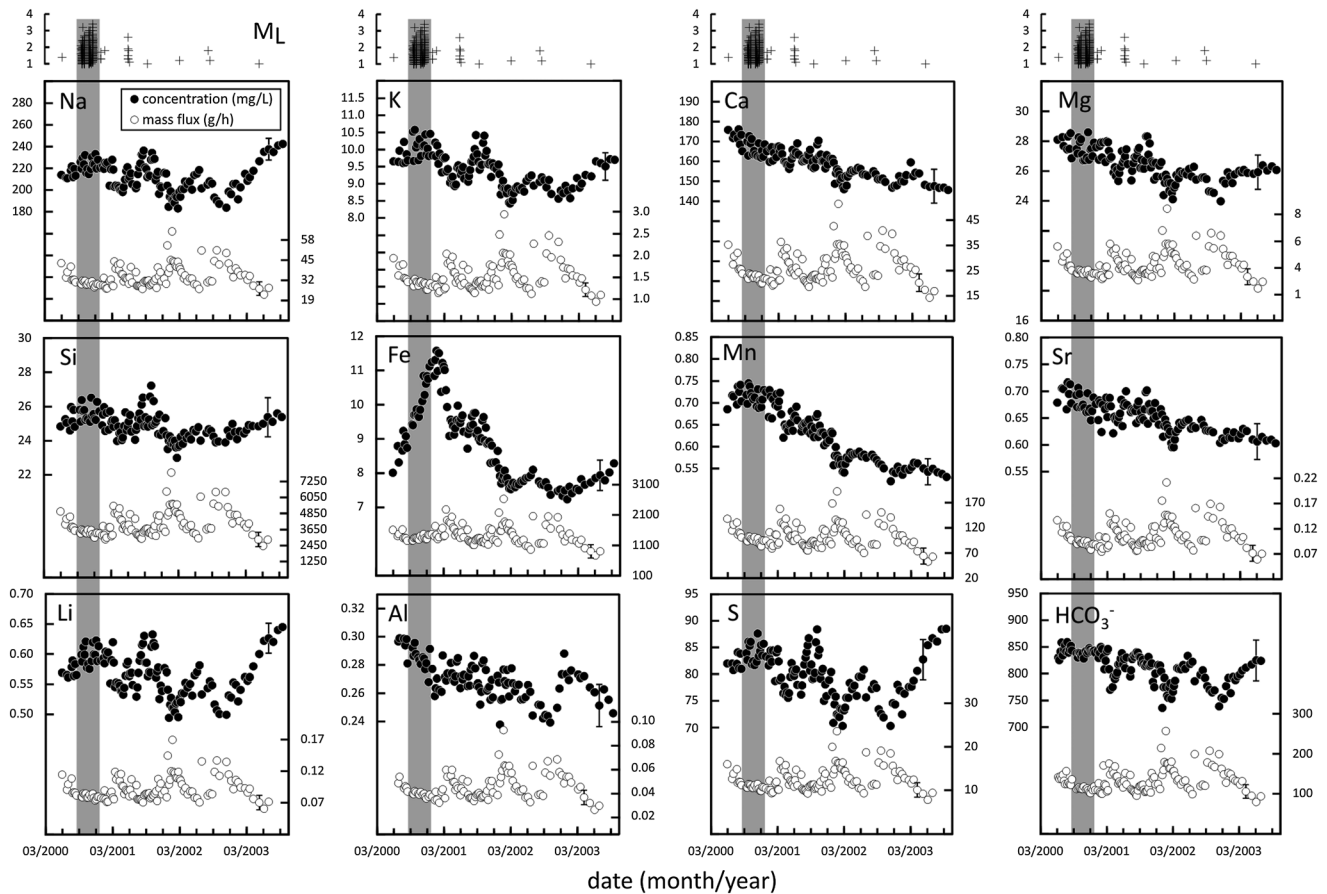


**Figure 3.** Time series data of mineral spring water chemistry from the Wettingquelle, Bad Brambach, Germany, between May 2000 and September 2003 for element concentrations (left axis, closed symbols, mg/L), and element mass fluxes (right axis, open symbols, g/h) as a function of time (date: month/yr). Mass fluxes are calculated by multiplication of concentrations with discharge (see Figure 5). Representative error bars for concentration and mass flux data are maximum uncertainty estimates. Discharge and  $\text{HCO}_3^-$  data from Bräuer *et al.* [2007]. The top panels show seismic activity in the Nový Kostel area with a local magnitude  $M_L > 1$  (data from WEBNET GFU Prague, <http://www.igg.cas.cz>). The vertical grey bands indicate the period of the strong earthquake swarm ( $M > 3$ ) period from the end of August 2000 to the end of January 2001.

Mg, Li, and S) show negative trends with increasing discharge (Figure 4), if the entire sampling period (2000 to 2003) is considered. This trend is corroborated by negative trends of conductivity (Figure 5e, data for conductivity from Bräuer *et al.* [2007]) with increasing discharge—at first view typical for a dilution effect [Koch and Heinicke, 2011]. For some elements like Na, K, Si, Mg, Li, S, and bicarbonate, this trend is more pronounced than for other elements like Ca, Fe, Mn, Sr, and Al. A more detailed view on the data from the time period 3 month before and after the strong 2000 swarm events (May 2000 to March 2001) shows that the data generally tend to cluster toward higher concentrations and lower discharge values in this period. However, no distinct trend in the concentration versus discharge pattern is discernable compared to the time period from March 2001 to December 2003. Even for Fe concentrations, where the data may indicate a weak negative trend with discharge during May 2000 to March 2001 (Figure 4), the observation is not compatible with typical trends expected for a simple dilution effect [Koch and Heinicke, 2011].

Iron isotope data of mineral spring water samples show a range in  $\delta^{56}\text{Fe}$  values from  $+0.06 \pm 0.05$  to  $-0.30 \pm 0.05\text{‰}$  (mean:  $-0.09 \pm 0.19\text{‰}$ , 2SD,  $n = 20$ , Table 1), with no indication of mass-independent isotope fractionation [Amor *et al.*, 2016] between  $\delta^{56}\text{Fe}$  and  $\delta^{57}\text{Fe}$  values (Table 1). Before and during the strong seismic swarm period ( $M_L > 3$ , starting in August 2000), coinciding with the development of anomalies in methane gas concentrations and  $\delta^{13}\text{C}_{\text{CH}_4}$  [Bräuer *et al.*, 2005],  $\delta^{56}\text{Fe}$  values are less variable ( $-0.01 \pm 0.11\text{‰}$ , 2SD,  $n = 4$ ) compared with the following period from 2001 to 2003 ( $-0.11 \pm 0.19\text{‰}$ , 2SD,  $n = 16$ ). In the latter period, intermittent events of low  $\delta^{56}\text{Fe}$  values down to  $-0.3\text{‰}$  are observed with a certain lag time after recurring seismic events ( $M_L > 1$ ). We have identified at least five significant negative

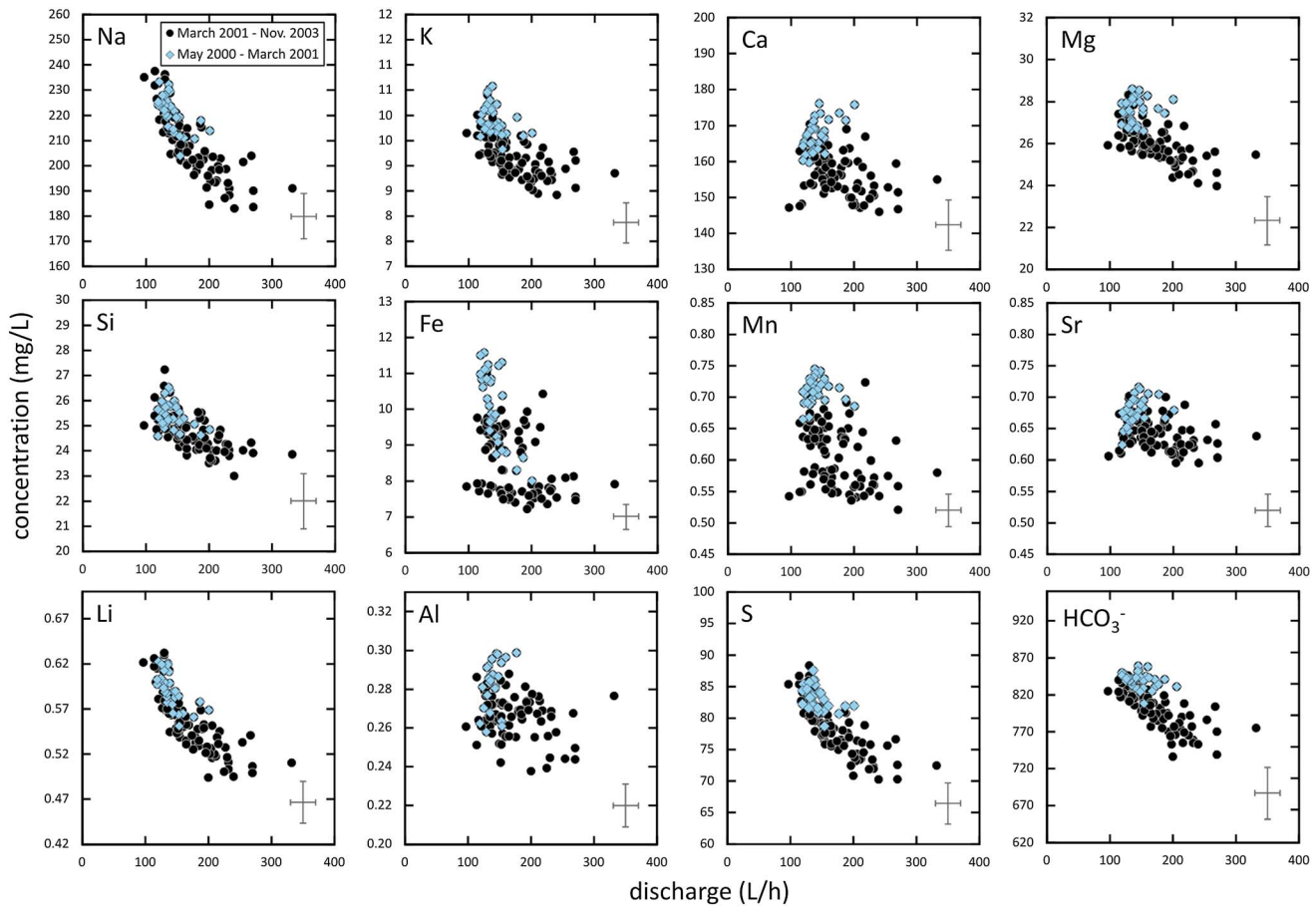
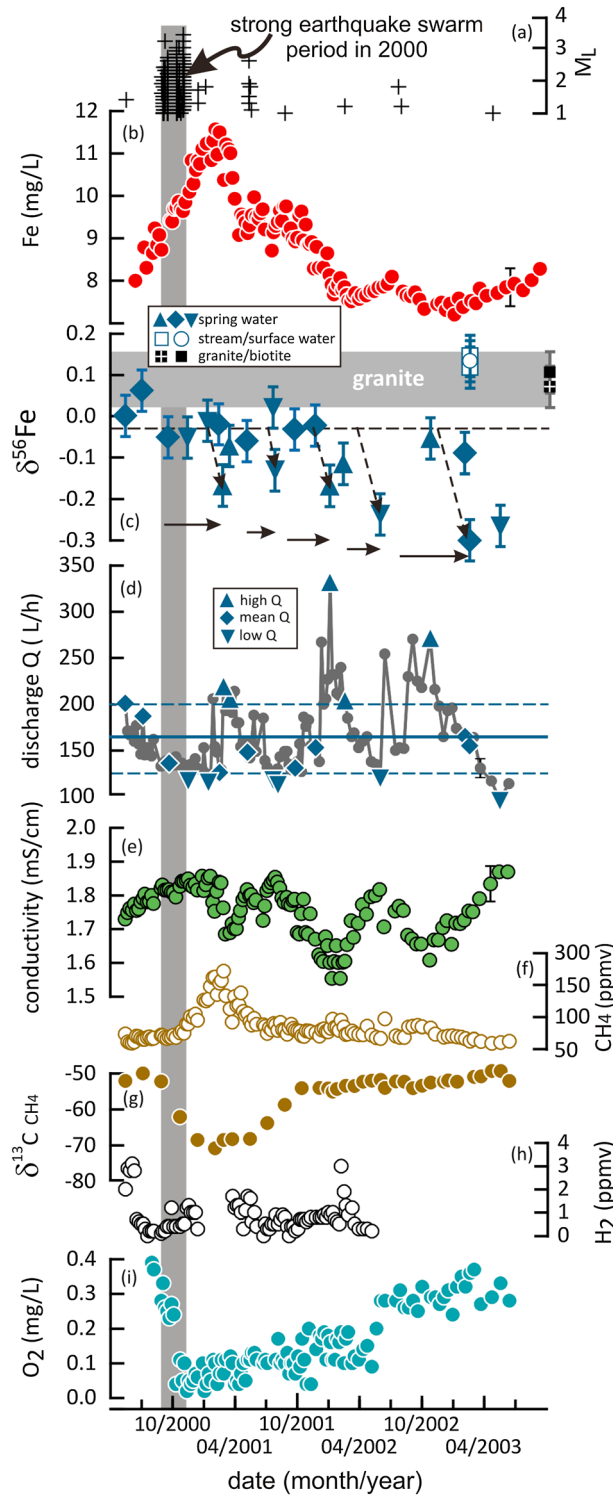


**Figure 4.** Element concentrations (mg/L) in Wettingquelle mineral water chemistry as a function of discharge (L/h). Light blue diamonds represent data from the time period 3 month before and after the strongest ( $M_L > 3$ ) swarm event (May 2000 to March 2001). Black solid circles are data from the postseismic period between March 2001 and November 2003. Representative error bars show maximum uncertainty estimates for both, concentration and discharge data. Discharge and  $\text{HCO}_3^-$  data from Bräuer *et al.* [2007].

anomalies in the time series data set (Figure 5c). In between,  $\delta^{56}\text{Fe}$  values of spring water return to a “baseline” value, characteristic for seismically quiet periods (Figure 5c and Table 1). This baseline  $\delta^{56}\text{Fe}$  value is not straightforward to determine due to irregular reoccurrence of seismic activity. In particular, direct selection of data points from seismically quiet periods cannot be applied due to the time lag between seismic events and Fe isotope response. Hence, we define the baseline  $\delta^{56}\text{Fe}$  value of  $-0.03 \pm 0.08\text{‰}$  (2SD,  $n = 8$ , Figure 5c), as the mean  $\delta^{56}\text{Fe}$  value of all mineral spring water samples that are identical within uncertainties to the two samples measured in May and June 2000, i.e., before the strong earthquake swarm. We chose this approach to acknowledge a small natural variability in  $\delta^{56}\text{Fe}$ , which might not be related to earthquake activity. Hence, our method is a conservative approach, detecting only the most significant negative  $\delta^{56}\text{Fe}$  deviations from the pre-earthquake baseline.

The water samples from the Röthenbach creek (30 m N of Wettingquelle spring, Figure 2) and an outflow of near-surface groundwater (outcrop spring, 200 m W of the Wettingquelle spring) are distinct to the deep sourced mineral spring water of the Wettingquelle in both element concentrations and  $\delta^{56}\text{Fe}$  values. The element concentrations are generally much lower than in the spring water (Table 1) and  $\delta^{56}\text{Fe}$  values of the dissolved Fe in all samples are undistinguishable (mean  $\delta^{56}\text{Fe} = +0.13 \pm 0.03\text{‰}$ , 2SD,  $n = 3$ , Table 1). The Fichtelgebirge granite sample is within the range of previously reported rock major element chemistry for this area (Table 2) with  $\text{SiO}_2$  contents typically ranging from 72.6 to 73.9 wt % and  $\text{Fe}_2\text{O}_3$  (total) between 0.56 and 1.6 wt % [Hecht *et al.*, 1997]. The major mineralogy comprises quartz, K-feldspar, plagioclase, biotite, and muscovite with accessories of apatite, zircon, monazite, uraninite, xenotime, thorite, and secondary chlorite and sericite [Förster, 1998; Hecht *et al.*, 1997]. Biotite is the major Fe-bearing phase (about 3 vol %



modal abundance in the granite) and has an identical (within analytical uncertainties)  $\delta^{56}\text{Fe}$  value of  $+0.07 \pm 0.05\text{‰}$  compared to the bulk rock ( $+0.11 \pm 0.05\text{‰}$ , Table 2).

#### 4. Discussion

The major source of Fe in the mineral spring water and its isotope composition is governed by the deep granite. This isotope signature is fractionated by a mixture of biotic and abiotic processes at depth and in the shallow aquifer (Figure 2). These processes result in lower  $\delta^{56}\text{Fe}$  values in the water compared to the granitic source (Figure 5). Evidence for this conclusion can be derived by considering the different processes in the aquifer and their con-

**Figure 5.** Time series data of the Wettingquelle mineral spring, Bad Brambach, between May 2000 and September 2003. (a) Seismic activity in the Nový Kostel area with a local magnitude  $M_L > 1$  (data from WEBNET GFU Prague <http://www.ig.cas.cz>). The vertical grey band indicates the period of the strong earthquake swarm period ( $M > 3$ ) from the end of August 2000 to the end of January 2001. (b) Dissolved Fe concentrations in spring water. (c) Fe isotope values of dissolved Fe in mineral spring water (closed symbols). Open symbols refer to surface water (circle) and stream water (squares) of the nearby Röthenbach creek (compare Figure 2). The grey horizontal band indicates the Fe isotope composition of granite bedrock, determined from analyses of bulk granite and biotite (black squares). The oblique arrows highlight negative  $\delta^{56}\text{Fe}$  anomalies, which are significantly different from the preseismic baseline signature of the mineral spring water (horizontal dashed line). The solid horizontal arrows indicate the lag time between a seismic event (Figure 5a) and the Fe isotope response in the water. (d) Mineral spring water discharge. High and low discharge (Q) values are defined as being outside the mean  $\pm$  SD of all data ( $164 \pm 39$  L/h), indicated by horizontal lines. (e) Conductivity of mineral spring water [from Bräuer et al., 2007]. (f and g) Methane concentrations in the free gas phase and the associated methane  $\delta^{13}\text{C}$  values [from Bräuer et al., 2007]. (h)  $\text{H}_2$  concentrations in gas [Bräuer et al. [2007]]. (i)  $\text{O}_2$  concentration in mineral spring water. For all data series where no error bar is shown the uncertainty is smaller than the symbol size.

**Table 2.** Analytical Results of the Fichtelgebirge Granite<sup>a</sup>

Sample (Analytical Method)	SiO <sub>2</sub> (wt %)	TiO <sub>2</sub> (wt %)	Al <sub>2</sub> O <sub>3</sub> (wt %)	Fe <sub>2</sub> O <sub>3</sub> (t) (wt %)	MgO (wt %)	CaO (wt %)	Na <sub>2</sub> O (wt %)	K <sub>2</sub> O (wt %)	MnO (wt %)	P <sub>2</sub> O <sub>5</sub> (wt %)	H <sub>2</sub> O (wt %)	CO <sub>2</sub> (wt %)	Ba (μg/g)	Sr (μg/g)	δ <sup>56</sup> Fe (‰)	δ <sup>57</sup> Fe (‰)
FG1 granite bulk rock (XRF)	73.1	0.21	14.6	1.24	0.32	0.60	3.2	5.3	0.02	0.30	0.92	0.06	251	66		
FG1 granite bulk rock (ICP-OES)	73.4	0.23	15.2	1.33	0.35	0.64	3.5	5.5	0.02				269	57	0.07	0.11
FG1m biotite from granite (ICP-OES)	32.7	3.1	20.5	27.0	6.4	<0.4	<0.5	7.5	0.40				202	<35	0.11	0.14
<i>Results From Hecht et al. [1997]</i>																
G1S granite bulk rock	72.6	0.27	14.6	1.60	0.45	1.03	4	4.8	0.033				568	95		
G1S granite bulk rock	73.4	0.13	14.5	1.07	0.24	0.53	3	4.8	0.021				123	26		
G1Sm granite bulk rock	73.9	0.07	14.6	0.56	0.07	0.44	4	4.3	0.024				42	24		

<sup>a</sup>Uncertainties (2SD) are better than 10% relative for concentration data. For Fe isotope data uncertainties are 0.05‰ (2SD) and 0.07‰ (2SD) for δ<sup>56</sup>Fe and δ<sup>57</sup>Fe, respectively. See supporting information Text S1 for analytical details.

nection to seismic events. In the following we discuss the role of (i) dissolution of Fe from the granite at depth and (ii) processes in the shallow oxygenated aquifer, where weathering and precipitation of secondary minerals as well as activity of Fe-metabolizing bacteria become more important.

#### 4.1. Fe Isotope Signatures Produced in the Deep Fractured Granite

The Wettingquelle mineral spring is located in a tectonically active zone characterized by strongly fractured granite. The water reaches the surface along fractures and fissures. The high CO<sub>2</sub> (2645 ± 203 mg/L) and HCO<sub>3</sub><sup>−</sup> concentrations (813 ± 57 mg/L) [Bräuer et al., 2007] allow carbonic acid to readily react with the rock during transport along fractures, dissolving minerals, therefore leading to the highly mineralized spring waters (total dissolved solids (TDS) up to 1.4 g/L) [Koch et al., 2005; Koch and Heinicke, 2011].

To explain the Fe isotope composition of the mineral spring water, we first assess the δ<sup>56</sup>Fe value of the granite bedrock from the bulk rock and biotite mineral analyses (Table 2). Both results for δ<sup>56</sup>Fe (+0.07 ± 0.05‰ and +0.11 ± 0.05‰) are identical within analytical uncertainties. This observation together with the knowledge on the mineralogical composition (see section 3) indicates that biotite is the major source of Fe in the granite. Our results are also consistent with the range reported for terrestrial bulk igneous rocks (δ<sup>56</sup>Fe = +0.09 ± 0.1‰), which is extended up to values of +0.38‰ for some highly evolved granites with SiO<sub>2</sub> above 71 wt % [Heimann et al., 2007; Poitrasson and Freyrier, 2005]. Although we have no direct evidence for metal-rich ore deposits in the deep Fichtelgebirge granite at our study site, hints from local secondary U-Ra enrichments exist [Koch et al., 1992; Watznauer and Koch, 1989], being responsible for the high radioactivity of the mineral spring water (up to 27 kBq/L). Moreover, granite-hosted ore deposits are abundant in the Erzgebirge mining district [Förster, 1999] located at the northern margin of the Bohemian Massif, where the Fichtelgebirge granite is situated. Hence, we cannot completely exclude the possibility of mineralized veins as an additional source of iron. Ore minerals (hematite, goethite, siderite, and Fe-Cu-sulfides) are expected to be isotopically fractionated and highly variable in δ<sup>56</sup>Fe (e.g., −2.3‰ to +1.3‰ measured in ore minerals from the Schwarzwald, Germany) [Markl et al., 2007].

Figure 5c illustrates that the typical granite-sourced Fe isotope signature is close to the measured δ<sup>56</sup>Fe values in the Wettingquelle water; however, significantly more negative δ<sup>56</sup>Fe values down to −0.3‰ are recurring. Can this Fe isotope signature be explained by deep abiotic fluid/rock interaction? During rock or mineral dissolution, faster dissolution rates of light isotopes at mineral surfaces can cause isotope fractionation during initial dissolution stages at high fluid to rock ratios. Leaching experiments of hornblende and granite bulk rock produced fluids that were isotopically lighter down to −1.8‰ in δ<sup>56</sup>Fe compared to the solid starting materials [Brantley et al., 2004; Chapman et al., 2009]. Once steady state conditions were reached after about 10 h, however, the leaching experiments of Fe from granite by hydrochloric and oxalic acid showed a decrease in isotopic fractionation relative to the bulk granite (−0.6 and −1‰, respectively) [Chapman et al., 2009]. The authors explain this behavior by alteration of biotite to chlorite and subsequent chlorite dissolution. This process is associated with precipitation of secondary minerals and adsorption/coprecipitation of Fe onto mineral surfaces upon oxalic acid dissolution. These findings can be applied to understand the deep granite dissolution processes at our study site. Analogously to the experiments, the Fichtelgebirge granite contains biotite as the main Fe-bearing mineral, which also undergoes

partial alteration to chlorite [Förster, 1998]. Hence, fluid rock interaction in the deep granitic Wettingquelle aquifer is expected to produce isotopically light Fe dissolved in water.

Notably, this trend toward negative  $\delta^{56}\text{Fe}$  in water is expected to be the same if potential ore mineral veins are acting as Fe source as they are dissolved. Dissolution of Fe-Mn oxides and Fe sulfides or Fe carbonates by interaction with reduced water (measured Eh values in the mineral spring water are around 107 mV) [Wagner *et al.*, 2007] is expected, where Mn(III,IV) and Fe(III) reduction results in release of Mn(II) and also ferric Fe into solution [Schuth *et al.*, 2015]. Hence, this process of dissolving minerals with predominantly negative  $\delta^{56}\text{Fe}$  values [Markl *et al.*, 2007] would also produce isotopically light Fe in water. However, due to variable  $\delta^{56}\text{Fe}$  values of ore minerals ( $-2.3\text{‰}$  to  $+1.3\text{‰}$ ), as discussed above, a precise prediction of the resulting Fe isotope signature of dissolved Fe upon reductive mineral dissolution is not possible.

As we have identified several potential mechanisms to create a deep source of isotopically light Fe, we can explore the possibility of mixing of different water sources facilitated by earthquake activity due to opening of new pathways for water in the subsurface, as previously observed [e.g., Poitrasson *et al.*, 1999; Toutain *et al.*, 2006; Woith *et al.*, 2013; Skelton *et al.*, 2014; Bachura and Fischer, 2016]. Here we test if a simple two-end-member mixing of varying amounts of water from the surface ( $\delta^{56}\text{Fe} = +0.13 \pm 0.03\text{‰}$  2SD,  $n = 3$ , Table 1) with highly mineralized water from the deep granite aquifer can explain the negative anomalies observed in the Fe isotope data set (Figure 5c). Investigations by Koch *et al.* [2005] and Koch and Heinicke [2011] found that the fraction of deep water (derived from tritium measurements) contributing to the Wettingquelle varies as a function of hydrological conditions, which correlate with conductivity ( $\lambda$ ), total dissolved solids (TDS), and discharge (Q). Therefore, we have systematically analyzed samples during high, low, and intermediate discharge periods for any correlation of  $\delta^{56}\text{Fe}$  with hydrochemical parameters (Figures 5c and 5d). However, the measured negative  $\delta^{56}\text{Fe}$  values do not always coincide with high discharge. Also, low discharge samples do not always have the most positive  $\delta^{56}\text{Fe}$  values, as would be expected from a simple mixing process of deep water (low Q and  $\delta^{56}\text{Fe}$  and high  $\lambda$  and TDS) with near-surface water (high Q and  $\delta^{56}\text{Fe}$  and low  $\lambda$  and TDS) [Koch *et al.*, 2005; Koch and Heinicke, 2011]. We modeled the temporal change in  $\delta^{56}\text{Fe}$  in a binary mixing model of deep water with surface water constrained by the measured Fe concentrations and isotopic compositions and hydrological mixing parameters from Koch *et al.* [2005]. However, no single realistic scenario can explain the variability of the Fe isotope data over the entire investigated period, in particular, due to the limited changes in surface water contributions relative to the deep water source (10–20%, see details on mass balance models in the supporting information Text S2). Hence, we conclude that a simple binary mixing of old deep water with young surface water, controlled by meteorological influences such as rainfall, snow melting, and atmospheric pressure, is not the first-order mechanism governing the variations in  $\delta^{56}\text{Fe}$  of the spring water. Therefore, we have to explore other mechanisms.

Remarkably, the most negative  $\delta^{56}\text{Fe}$  values are found in water samples that have the lowest Fe and the highest oxygen concentrations, respectively (Figures 6b and 6d). Notably, no overall statistically significant correlation between Fe concentration (or Fe mass flux) and isotope ratios ( $\delta^{56}\text{Fe}$  and  $\delta^{13}\text{C}$ ) or gas content ( $\text{H}_2$  and  $\text{O}_2$ ) in the water is observed when the entire data set (2000–2003) is considered (Figure 6). However, no such correlation is expected in the data set comprising seismically active and quiet periods. This is due to the observed temporal decoupling of cause and effect, i.e., earthquake forcing and response in hydrochemical and isotopic signals (discussed in more detail in the conceptual model below, section 4.4). These observations are consistent with the time series trends in these data. Specifically,  $\text{O}_2$  content in the water decreases before and during the strong earthquake swarm around October 2000 (Figure 5i), whereas Fe concentration increases (Figure 5b). Moreover, the postseismic trend after the strong swarm event in 2000 is characterized by a slow and steady increase in  $\text{O}_2$  and a decrease in Fe concentration from 2001 to 2003. During this period the weak negative correlation between Fe concentration and discharge also disappears (Figure 4), indicating that other than simple discharge dilution effects become important, as discussed above, and consistent with previous hydrological observations [Koch *et al.*, 2005; Koch and Heinicke, 2011]. Accordingly, this apparently coupled behavior of Fe and  $\text{O}_2$  suggest that redox processes are involved, consistent with the absence of such trends in nonredox elements, for example, Na or Si (Figure 3). Fe isotopes are sensitive to redox processes, where oxidation of  $\text{Fe(II)}_{\text{aq}}$  to  $\text{Fe(III)}_{\text{aq}}$  (and subsequent precipitation of  $\text{Fe(III)(hydr)oxides}$ ) is associated with enrichment of isotopically light Fe in the water (see processes discussed in the next section). More negative  $\delta^{56}\text{Fe}$  values are indeed observed in the late observation period in 2002–2003 (Figure 5c),

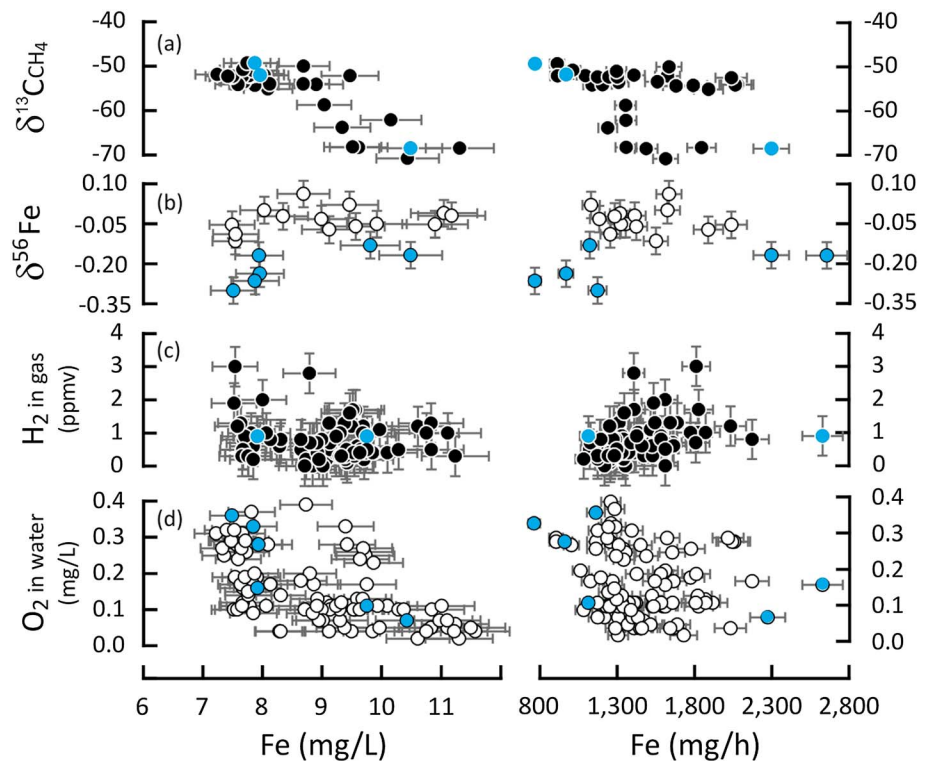


**Figure 6.** (a)  $\delta^{13}\text{C}$  values of methane [Bräuer *et al.*, 2007] and (b)  $\delta^{56}\text{Fe}$  values of mineral spring water (c)  $\text{H}_2$  concentration in gas [Bräuer *et al.*, 2007], (d)  $\text{O}_2$  concentration in water as a function of Fe concentration in water and Fe mass flux (derived from Fe concentration multiplied with discharge). Samples showing postseismic negative  $\delta^{56}\text{Fe}$  anomalies in mineral spring water (compare Figure 5c) are color coded as blue filled circles (note that not all parameters were analyzed for all samples).

where oxygen contents are higher, promoting inorganic oxidation reactions. We note that we do not have direct statistical evidence for the control of  $\text{O}_2$  on Fe isotope signatures in the spring water. However, as mentioned above, such correlations are challenging to extract from the data set obtained in this complex geodynamic environment. Nevertheless, as we do not have evidence against a redox control on  $\delta^{56}\text{Fe}$  values, we still have to consider this mechanism. Hence, in the following we discuss the impact of redox reactions in the oxygenated shallow aquifer on Fe isotopes in mineral spring water.

#### 4.2. Processes in the Shallow Oxygenated Aquifer

In addition to rock dissolution, also, secondary mineral formation from the  $\text{CO}_2$ - and metal-rich waters can have an impact on the Fe isotope composition of dissolved Fe in the spring water. At depth, under reducing conditions, ferrous iron is mobile and transported upward in dissolved form. Oxygen can only enter the system in the vicinity of the spring capture with the 10–20% young water, i.e., within the last meters below the spring capture. Here oxygenated water is mixed into the aquifer, causing precipitation of Fe(III)-bearing oxides and (oxy)hydroxides, which can be observed also at the spring capture, and secondary amorphous precipitates have been documented in the fractured granite [Heinicke *et al.*, 2009]. These phases are expected to be isotopically heavier compared to aqueous Fe by 0.1 to 0.4‰ in  $\delta^{56}\text{Fe}$  for equilibrium isotope fractionation [Saunier *et al.*, 2011; Skulan *et al.*, 2002] or by up to about 1‰ for combined kinetic and equilibrium fractionation [Bullen *et al.*, 2001], leaving behind an isotopically lighter water, which moves farther toward the Wettingquelle spring capture. Due to the high  $\text{CO}_2$  content of the water, potential siderite formation also has to be considered. The isotopic fractionation during precipitation of siderite from  $\text{Fe(II)}_{\text{aq}}$  was predicted from spectroscopic data, where siderite is approximately  $-1.5\text{‰}$  lighter than dissolved iron [Polyakov and Mineev, 2000], consistent with experimental findings ( $\Delta^{56}\text{Fe}_{\text{siderite}-\text{Fe(II)}_{\text{aq}}}$  of  $-0.5\text{‰}$ ) [Wiesli *et al.*, 2004]. The estimated change in  $\delta^{56}\text{Fe}$  values in the water by precipitation of solids from the water can be assessed by a simple mass balance model calculation. Mass balance predicts that uptake of isotopically heavy Fe from

solution into precipitating solids, and the related depletion in heavy isotopes in the water, is detected in the dissolved  $\delta^{56}\text{Fe}$  only when the associated mass transfer of Fe is large enough—but not complete. A closed system or Rayleigh-type mass balance model (e.g., see review by *Wiederhold* [2015]) can be used to estimate the relative change in dissolved Fe concentrations. The actual combined isotope fractionation factor of combined precipitation of Fe(III)(oxy)hydroxides and Fe(II)carbonates is not known precisely, because the relative proportions of the two phases are not known. However, using a fractionation factor for pure siderite formation, i.e.,  $\Delta^{56}\text{Fe}_{\text{siderite-Fe(II)aq}}$  of  $-0.5\text{‰}$ , [*Wiesli et al.*, 2004], in the model does not reproduce the measured range in  $\delta^{56}\text{Fe}$  values in the water and is therefore considered unlikely. Hence, to estimate a minimum change in dissolved Fe concentrations, a conservative maximum  $\Delta^{56}\text{Fe}_{\text{solid-solution}} = 1\text{‰}$  [*Bullen et al.*, 2001] for predominately Fe(III)(oxy)hydroxides formation is used and a granite-like Fe isotope signature (0.09‰) of the starting solution. The model results show that at least 17 to 39% Fe removal from the water is required to be consistent with the  $\delta^{56}\text{Fe}$  values measured in the Wettingquelle mineral spring water (Table 1), for both a closed system and Rayleigh-type mass balance model. Hence, the model results predict a change in the dissolved Fe concentration in water to values of 6.8 to 9.3  $\mu\text{g/mL}$  Fe, assuming the starting Fe concentration is close to the maximum measured value of 11.1  $\mu\text{g/mL}$  Fe (Table 1), which might actually be slightly higher but is unknown. Although no overall correlation is found between Fe concentration or Fe mass flux and  $\delta^{56}\text{Fe}$ , we can see from Figure 6b that the samples with the lowest Fe concentrations or Fe mass flux indeed have the most negative  $\delta^{56}\text{Fe}$  values and the measured Fe concentrations are in a similar range than the model predictions. Notably, changing the combined isotope fractionation factor from  $\Delta^{56}\text{Fe}_{\text{solid-solution}} = 1\text{‰}$  to  $< 0.5\text{‰}$  would result in Fe concentration in the water of less than 7  $\mu\text{g/mL}$  Fe, which is not observed (Figure 5b), and therefore, our choice of 1‰ is considered reasonable. Again, we stress that no overall correlation between Fe concentration and  $\delta^{56}\text{Fe}$  is expected in the data set comprising seismically active and quiet periods, due to the temporal decoupling of earthquake forcing and response in hydrochemical and isotopic signals (Figure 6b). Moreover, efficient oxidation of  $\text{Fe(II)}_{\text{aq}}$  and subsequent precipitation of isotopically heavy Fe(III)(oxy)hydroxides is likely in the oxygenated near-surface aquifer (Figure 2). Such conditions are indicated in Figure 6d, where the highest  $\text{O}_2$  concentrations in the water coincide with the lowest Fe concentrations (i.e.,  $< 8 \text{ mg/L}$ ) and, again, the lowest  $\delta^{56}\text{Fe}$  values. Hence, we suggest that precipitation of Fe(III)-bearing phases from the water is supported in the shallow aquifer system and is a potential mechanism to further deplete the ascending deep water in isotopically heavy Fe, which already has a  $\delta^{56}\text{Fe}$  signature lower than the bulk granite as discussed above (see section 4.1).

In summary, we have identified abiotic processes in both the deep and the shallow aquifer that are able to generate the iron isotope signatures observed in the spring water. In the following, we explore possible biotic influences on Fe isotopes.

### 4.3. Microbial Impact on Fe Isotope Signatures

Some microorganisms can grow in habitats with very low concentrations of organic compounds as long as other energy sources are available [*Kietavainen and Purkamo*, 2015]. Mineral waters are such a habitat. The  $\delta^{13}\text{C}$  isotopic signature of methane at Wettingquelle might be of microbial origin, with admixture of thermogenic/abiogenic formed methane (shallow and/or deeper granitic source) with minor contributions from upper mantle methane [*Bräuer et al.*, 2005; *Bräuer et al.*, 2007]. The onset of the sharp rise in the methane concentration was observed just 8 weeks after the start of the strong swarm earthquake period at the end of August 2000 (Figure 5a). The coseismic decrease in the methane  $\delta^{13}\text{C}$  values and correlated increase in methane concentrations (Figures 5f and 5g) lead to the suggestion of a microbial methane origin, supported by spikes in hydrogen concentrations (Figure 5h) released from the fissured granite. Then, autotrophic methanogens produce methane from hydrogen and  $\text{CO}_2$ . At our study site, generally two different hypotheses can explain the increase of  $\text{H}_2$  related to seismic activity. One is based on radioactive minerals that support generation of hydrogen by radiolysis [*Bräuer et al.*, 2005], the other assumes a reaction of  $\text{H}_2\text{O}$  with radicals on freshly formed rock fractures [*Ito et al.*, 1999, and references therein].

*Wagner et al.* [2007] characterized the bacterial communities in the deep aquifer of the Wettingquelle water sampled 23 months after the strong earthquake swarm in 2000. Close relatives of *Gallionella ferruginea* [*Hallbeck et al.*, 1993], a micro aerobic oxidizer of ferrous iron, was the most abundant bacterial group. Minor occurrences of bacterial groups related to *Geothrix fermentans* [*Coates et al.*, 1999], iron reducers and nitrite oxidizers, as well as relatives of *Thiobacillus* [*Robertson and Kuenen*, 2006], aerobic sulfur reducers,

and members of the *Sulfuricum*-cluster [Kodama and Watanabe, 2004], sulfur oxidizers, were found. Detection of known iron oxidizers and iron reducers indicates the importance of microbial iron utilization in this aquifer. These bacterial groups of known physiology depend on reduced compounds from depth and on oxygen supplied by the younger surface water, entering in the vicinity of the spring capture [Wagner et al., 2007]. Hence, a biological control on the Fe isotope signature in the shallow spring water needs to be considered.

Several studies found Fe isotope fractionation in aqueous systems during biologically mediated reactions in presence of different species with specific Fe-utilization mechanisms. During dissimilatory iron reduction, bacteria, such as *Shewanella putrefaciens*, *Geobacter sulfurreducens*, and *Geothrix fermentans*, reduce Fe (III)-bearing solid phases and isotopically light Fe is released into solution [Beard et al., 1999; Crosby et al., 2007]. Croal et al. [2004] showed that photoautotrophic and phototrophic bacteria (*Thiorhodaceae*, *Thiodictyon*, and *Chlorobium ferrooxidans*) oxidize aqueous Fe(II) and combined with subsequent precipitation of Fe(III)(oxy)hydroxides also produce an isotopically light signature in the solution. Other studies, for example, investigated nitrate-reducing Fe(II)-oxidizing bacteria (*Acidovorax* sp.), siderophores-producing oxygen-respiring heterotrophic bacteria (*Bacillus* sp. and *Streptomyces* sp.), and Fe adsorption onto planktonic cyanobacteria (*Gloeocapsa* sp., *Synechococcus* sp., and *Planthothrix* sp.) [Brantley et al., 2004; Kappler et al., 2010; Mulholland et al., 2015]. Overall, previous studies indicate that bacterially mediated Fe isotope fractionation ultimately results in an aqueous solution that is isotopically lighter by  $-0.6$  to  $-3\%$  in  $\delta^{56}\text{Fe}$  compared to the Fe source.

The clear identification of such biotic Fe isotope signatures in water samples of the Wettingquelle is challenging. This is because most of the described biological processes are governed by the same fundamental physical and chemical principles as abiotic processes. Fe isotope fractionation occurs during redox reactions and also by catalyzing coupled atom and electron exchange, complexation, sorption, and diffusion reactions. In a complex aquifer system like the one feeding the spring at Wettingquelle, we can neither confirm nor exclude the role of biological influence on processes in the aquifer based on our data. Although the postseismic negative values in  $\delta^{56}\text{Fe}$  cannot be unambiguously ascribed to pure abiotic or biotic processes, we can still discuss these events (and the combination of both) in the framework of recurring seismic forcing and response of biogeochemical processes.

#### 4.4. Conceptual Model: Tectonic Forcing on Biogeochemical Processes

Bräuer et al. [2007] used the response of gas compositions ( $\delta^{13}\text{C}_{\text{CO}_2}$  and  $^3\text{He}/^4\text{He}$ ) emanating at the Wettingquelle after the seismic events in 2000 and in 1994 at the Eisenquelle, Bad Brambach (located approximately 75 m WNW of the Wettingquelle) [Weise et al., 2001] to estimate the fluid transport velocity and the lag time of fluids ascending from the hypocenter to the surface. The gas at the Wettingquelle responded after 60 to 100 days and a maximum lag time of about 300 days was estimated using the fluid transport velocity of 50 m/day for the nearby Eisenquelle [Weise et al., 2001]. Indeed, after the strong seismic activity, starting at the end of August 2000, a first negative  $\delta^{56}\text{Fe}$  anomaly deviating from the preseismic baseline ( $-0.03 \pm 0.08\%$  2SD,  $n=8$ , Figure 5c) is observed after approximately 195 days in the spring water on 14 March 2001 ( $\delta^{56}\text{Fe} = -0.17 \pm 0.05\%$ , Figure 5c). Subsequent negative  $\delta^{56}\text{Fe}$  anomalies are observed in the period from 2001 to 2003. For each negative  $\delta^{56}\text{Fe}$  anomaly a preceding seismic event ( $M_L > 1$ ) can be identified (Figures 5a and 5c), indicating variable lag times between tectonic forcing and Fe isotope response between 60 and 300 days (Figure 5c). This is consistent with fluid transport velocities from different hypocenter depths because new fractures are successively opening as a result of the upward migration of the swarm's foci along the steep fault structure [Bachura and Fischer, 2016; Fischer et al., 2014]. In between, related to seismically quiet periods, the  $\delta^{56}\text{Fe}$  values return to the baseline, closer to the granitic source signature. We explore two scenarios to explain the detailed Fe isotope fractionation mechanisms that are triggered by the seismic events—an abiotic and biotic one.

Considering purely abiotic reactions in the deep granitic aquifer, we suggest that upon tectonic fracturing, dilation and enhanced permeability, more intense fluid/rock interaction facilitates rock dissolution [e.g., Wasteby et al., 2014; Andr n et al., 2016], and newly generated reactive surface fronts are expected to release isotopically light Fe into the water as discussed above (see section 4.1). Because any initial Fe isotope fractionation due to removal of the first atomic layers of a mineral is a kinetic isotope effect that subsides after a



certain time [Brantley *et al.*, 2004; Chapman *et al.*, 2009], this isotopically light Fe is released as a temporally restricted pulse (Figure 5b). After a seismic event this is then admixed to the continuously produced baseline Fe isotope signature of dissolved Fe in the mineral spring water and Fe concentration increases (Figure 5b). This negative Fe isotope signal becomes only visible once mass balance favors the “low- $\delta^{56}\text{Fe}$  pulse” to dominate the Fe budget in the water at expense of the baseline  $\delta^{56}\text{Fe}$  signature (Figure 5c). At the same time, the abiotic precipitation of ferric (hydrated)oxides upon oxidation of ferrous iron transported by reduced fluids from depth toward the oxygenated shallow aquifer is also capable of generating additional temporally restricted negative Fe isotope signatures in the spring water. In particular, as a preseismic and coseismic increase in Fe concentration occurs (Figure 5b), these conditions (closer to Fe solubility limit) are favorable to support larger amounts of isotopically fractionated ferric (hydrated)oxides precipitation. Obeying Fe isotope mass balance, this fractionated signal of isotopically light Fe becomes visible in the water once a significant amount of solids precipitated (see mass balance considerations in section 4.2). The decay of the hydrochemical anomaly is controlled by fracture healing (rock alteration and precipitation of secondary minerals) in the granite aquifer, decreasing permeability, and is periodically interrupted by refracturing seismic events. Such a hydrochemical recovery mechanism was, for example, suggested from postseismic observations after  $M > 5$  earthquakes in Iceland [e.g., Wasteby *et al.*, 2014; Andr n *et al.*, 2016].

Moreover, in the shallow aquifer, where the geothermal gradient facilitates temperatures low enough to sustain microbial life ( $< 121^\circ\text{C}$ ) [Kashefi and Lovley, 2003], we suggest a seismically triggered scenario, where biotically mediated reactions involving Fe become important. To “activate” episodically amplified microbial activity, we need to consider essential conditions required for such reactions. First, to support microbial activity, different chemical compounds as a source of energy and carbon are needed—depending on the highly specialized metabolism of different microorganisms (see section 4.3). Mineralized water at Wettingen is a habitat providing ample supply of Fe and  $\text{CO}_2$  for iron-utilizing bacteria and methanogens, respectively. As some of these organisms also depend on  $\text{O}_2$ , the spring capture and the shallow aquifer, where  $\text{O}_2$  from surface water is admixed, support microbially mediated Fe reactions, which are associated with isotopic fractionation. Further, one limiting parameter for  $\text{H}_2$ -dependent methanogens in the deep subsurface is hydrogen supply [Kietavainen and Purkamo, 2015]. Though  $\text{H}_2$  is constantly supplied by radiolysis due to the presence of radioactive minerals [Br uer *et al.*, 2005], an additional peak in  $\text{H}_2$  supply can be expected by preseismically and coseismically induced opening of fractures that tap sealed deep  $\text{H}_2$  reservoirs, where  $\text{H}_2$  has accumulated over tectonically inactive periods. Subsequently, advective transport toward the surface occurs. Noteworthy, the connection between  $\text{H}_2$ -dependent methanogens and Fe-utilization has been found in certain bacteria that are able to switch between hydrogenotrophic methane production and ferric iron reduction, or even perform both reactions simultaneously [Sivan *et al.*, 2016].

In our biotically mediated Fe isotope fractionation scenario, increased hydrogenotrophic microbial activity is triggered by release of  $\text{H}_2$  during the preseismic and coseismic period (e.g., in May 2000, September 2000, and March 2002, Figure 5h). Methanogenesis starts after a certain lag time during which fluid transport and microbial growth occurs. This is evident by a sharp rise in  $\text{CH}_4$  concentration (e.g., a strong peak in March 2001, and smaller peaks in February 2002 and August 2002, Figure 5f) and anomalies in  $\delta^{13}\text{C}$  of methane (Figure 5g). Again, a temporal decoupling between seismic forcing and triggering of a subsequent chain reaction is indicated by the absence of straightforward correlations between Fe and  $\text{H}_2$  and Fe and  $\delta^{13}\text{C}$  of  $\text{CH}_4$  in the overall data set covering seismically active and quiet periods (Figures 6a and 6d). As large amounts of methane are produced, also, oxidation of  $\text{CH}_4$  begins. This can occur via aerobic methanotrophic bacteria by oxidation of  $\text{CH}_4$  to methanol and  $\text{CO}_2$ , using  $\text{O}_2$  as the electron acceptor or via the anaerobic oxidation of methane (AOM). During AOM methane is oxidized with various terminal electron acceptors such as sulfate, nitrate, nitrite, and metals such as iron [Hansen *et al.*, 1998; Hinrichs *et al.*, 1999; Hoehler *et al.*, 1994]. Microbial methane oxidation with iron and/or manganese reduction was first described in marine sediments [e.g., Beal *et al.*, 2009] but was later also found in a terrestrial mud volcano [Chang *et al.*, 2012] and freshwater environments [e.g., Amos *et al.*, 2012; Crowe *et al.*, 2011; Sivan *et al.*, 2011]. Indeed, a preseismic and coseismic decrease in  $\text{O}_2$  concentration is observed (Figure 5i) as well as a decay of the Fe and  $\text{CH}_4$  peaks (Figures 5b, 5f, and 5g). When oxygen is depleted, microbially mediated reduction of iron takes over. This process is not instantaneous but proceeds over a certain time period. This is consistent with the absence of an overall direct correlation between Fe and  $\text{O}_2$  (Figure 6d) in water considering the entire data set covering seismically active

and quiet periods. Instead, a temporal decoupling is indicated by the observation that recurring negative  $\delta^{56}\text{Fe}$  values in spring water are found after a time lag of at least 60 days after the occurrence of a seismic event (Figure 5c). Here two microbial communities, which were observed by Wagner *et al.* [2007], are potential drivers of isotopic fractionation. First,  $\text{Fe(II)}_{\text{aq}}$  oxidizing bacteria, like *Gallionella ferruginea* [Hallbeck *et al.*, 1993], are active in the oxygenated shallow aquifer [Wagner *et al.*, 2007], where—upon  $\text{Fe(II)}_{\text{aq}}$  oxidation to  $\text{Fe(III)}_{\text{aq}}$ — $\text{Fe(III)(oxy)hydroxides}$  are precipitated. This ultimately results in incorporation of isotopically heavy Fe in solid phases, leaving an isotopically light residue in the water, which slowly evolves toward lower Fe concentrations (Figure 5b). Second, the same isotopic effect is generated by the presence of ferric iron-reducing bacteria [Crosby *et al.*, 2007], i.e., the detected organism affiliated with *Geothrix fermentans* that thrive under anaerobic conditions at greater depth in the aquifer [Wagner *et al.*, 2007]. This also results in the release of isotopically light Fe into the water (see fractionation factors discussed in section 4.3) that is observed in the Wettingquelle spring water (Figure 5c). Mineral-bound iron, present in amorphous or poorly crystalline ferric hydrous oxide, is readily accessible to microbes as electron acceptor [Sivan *et al.*, 2016] and is typically amongst the first products of granite weathering together with secondary amorphous Si-Al precipitates in both deep fluid-filled fractures that can also be observed at the spring capture in the near-surface low-temperature weathering zone [Heinicke *et al.*, 2009] (Figure 2). Based on the observation that Fe concentrations in water start to increase before the strong seismic event (Figure 5b), we suggest that Fe-reducing bacteria operate at greater depth and are activated earlier by the preseismic dilation and  $\text{H}_2$  release (Figure 5h) compared to the microbial communities in the shallow oxygenated aquifer. Once the additional seismically induced  $\text{H}_2$  supply has been consumed (see decline to baseline values in Figure 5h), methanogenesis slows down, microbial activity ceases, and the  $\text{CH}_4$  concentration sharply declines (Figure 5f). This is consistent with an assessment of the stoichiometry of the methanogenesis reaction [Amend and Shock, 2001] with respect to measured  $\text{H}_2$  and  $\text{CH}_4$  concentrations (supporting information Text S3). Then, also microbially mediated Fe reduction ceases. Meanwhile, closer to the surface, Fe-oxidizing bacteria continue to oxidize  $\text{Fe(II)}_{\text{aq}}$ , which removes dissolved Fe from the water into  $\text{Fe(III)(oxy)hydroxides}$ , until the elevated Fe supply from depth is exhausted. This leads to a postseismic decrease in Fe concentration (Figure 5b). As a result microbial Fe utilization and the associated isotopic fractionation decline. This leads to a return of the  $\delta^{56}\text{Fe}$  values of spring water to a “baseline value,” dominated by the deep granite isotope signature (Figure 5c), until the next seismic event triggers the chain reaction.

We conclude that most likely a combination of both abiotic and biotic scenarios control the complex coupled biogeochemical processes in the aquifer that can generate distinct negative postseismic Fe isotope anomalies in the spring water arriving at the surface (Figure 5c). This is consistent with previous observations on biotic and abiotic Fe isotope fractionation during a field experiment in a groundwater well, where changes in redox conditions were imposed [Teutsch *et al.*, 2005].

To further constrain the proposed model, future time series investigations are needed that combine microbiological with isotope geochemical analyses on the exact same samples affected by recurring seismic events. Such studies can help to disentangle the relative contributions of abiotic and biotic processes.

## 5. Conclusions

Our objective was to test whether Fe isotopes trace earthquake-induced abiotic and biotic changes in the fluid/rock interaction of the deep fissured granitic aquifer. We observed that the Fe isotope data measured in mineral spring water of the Wettingquelle are on average lower compared to the granitic bulk rock signature. This can be explained by a mixture of mineral dissolution reactions at depth and potential precipitation of solids in tectonic fractures and in the shallow near-surface aquifer and the spring capture itself. Due to the complexity of biotic and abiotic processes, no characteristic Fe isotope fingerprint of deep biosphere activity promoted by earthquake activity can be identified unambiguously. Rather, a complex combination of inorganic and organic processes is likely to control the Fe isotope signature of spring water, where the deep granitic Fe source dominates the Fe isotope mass balance and is altered by intermittent seismic events producing distinct negative  $\delta^{56}\text{Fe}$  values. Strikingly, our data show a time lag between tectonic forcing and Fe isotope response recorded in spring water, indicating that earthquake-induced changes in the fluid/rock interaction and biogeochemical processes control Fe isotope signatures. In our model scenarios, we suggest that seismically released hydrogen activates the deep biosphere, where microbial utilization of Fe causes Fe

isotope fractionation. At the same time, fresh fractures open at depth, temporarily release isotopically light iron into water that ascends toward the surface. Then, it is mixed with water from the shallow oxygenated aquifer, where Fe is oxidized and subsequent ferric (hydrrous)oxide formation occurs. The combination of these abiotic and biotic processes is traced by the distinct Fe isotope signal measured in the mineral spring water.

#### Acknowledgments

We would like to thank Karin Bräuer (UFZ Helmholtz Centre for Environmental Research at Halle/Saale, Germany) for her continuous research efforts in the western part of the Eger Rift over 25 years. Her studies provided the foundation of the present study, including the long-term monitoring and time series water sampling at Wetzinquelle. Friedhelm von Blanckenburg (GFZ) is thanked for supporting this project and for discussions. J. Bartel, J. Buhk, A. Balduin, and G. Floor are acknowledged for laboratory support at GFZ. A. Gottsche (GFZ) is thanked for the granite XRF measurement. Further technical assistance was provided by P. Dulski and A. Hendrich at GFZ. Aurèle Vuillemin (GFZ), and the members of the GFZ Earth Surface Geochemistry group are thanked for fruitful discussions. The manuscript was improved thanks to the detailed and constructive reviews of K. van Zuilen and an anonymous reviewer. Despite serious efforts, we did not manage to integrate a joke into this paper. This research has been supported by coffee and the German Research Foundation (grants MA 1898/1, KA 902/7, and 16) and benefited from Helmholtz Association infrastructure funding at GFZ. All data used in this study are listed in the tables or in the supporting information. Wherever previously published data were used, references are indicated.

#### References

- Amend, J. P., and E. L. Shock (2001), Energetics of overall metabolic reactions of thermophilic and hyperthermophilic Archaea and Bacteria, *Fems Microbiol. Rev.*, *25*(2), 175–243, doi:10.1016/s0168-6445(00)00062-0.
- Amor, M., V. Bisigney, P. Louvat, A. Gelabert, P. Cartigny, M. Durand-Dubief, G. Ona-Nguema, E. Alphandery, I. Chebbi, and F. Guyot (2016), Mass-dependent and -independent signature of Fe isotopes in magnetotactic bacteria, *Science*, *352*(6286), 705–708, doi:10.1126/science.aad7632.
- Amos, R. T., B. A. Bekins, I. M. Cazzarelli, M. A. Voytek, J. D. Kirshtein, E. J. P. Jones, and D. W. Blowes (2012), Evidence for iron-mediated anaerobic methane oxidation in a crude oil-contaminated aquifer, *Geobiology*, *10*(6), 506–517, doi:10.1111/j.1472-4669.2012.00341.x.
- Anbar, A. D., A. A. Jarzecki, and T. G. Spiro (2005), Theoretical investigation of iron isotope fractionation between Fe(H<sub>2</sub>O)(3+)(6) and Fe(H<sub>2</sub>O)(2+)(6): Implications for iron stable isotope geochemistry, *Geochim. Cosmochim. Acta*, *69*(4), 825–837, doi:10.1016/j.gca.2004.06.012.
- Andr n, M., et al. (2016), Coupling between mineral reactions, chemical changes in groundwater, and earthquakes in Iceland, *J. Geophys. Res. Solid Earth*, *121*, 2315–2337, doi:10.1002/2015jb012614.
- Ardini, F., F. Soggia, F. Rugi, R. Udisti, and M. Grotti (2010), Comparison of inductively coupled plasma spectrometry techniques for the direct determination of rare earth elements in digests from geological samples, *Anal. Chim. Acta*, *678*(1), 18–25, doi:10.1016/j.aca.2010.07.036.
- Babuska, V., and J. Plomerova (2008), Control of paths of quaternary volcanic products in western Bohemian massif by rejuvenated Variscan triple junction of ancient microplates, *Stud. Geophys. Geod.*, *52*(4), 607–629, doi:10.1007/s11200-008-0040-0.
- Bachura, M., and T. Fischer (2016), Detailed velocity ratio mapping during the aftershock sequence as a tool to monitor the fluid activity within the fault plane, *Earth Planet. Sci. Lett.*, *453*, 215–222, doi:10.1016/j.epsl.2016.08.017.
- Baedecker, P. A. (1987), Methods for geochemical analysis, U.S. Geol. Surv. Bull., 1770 p.
- Bankwitz, P., G. Schneider, H. K mpf, and E. Bankwitz (2003), Structural characteristics of epicentral areas in Central Europe: Study case Cheb Basin (Czech Republic), *J. Geodyn.*, *35*(1–2), 5–32, doi:10.1016/s0264-3707(02)00051-0.
- Baumann, L., K.-H. Bernstein, H. K mpf, and P. Wolf (1982), Zur minerogenetischen Bedeutung von Bruchstrukturen am NW-Rand des B hmischen Massivs (Bereich Vogtland), *Zeitschrift f r Angewandte Geol.*, *28*, 463–470.
- Beal, E. J., C. H. House, and V. J. Orphan (2009), Manganese- and iron-dependent marine methane oxidation, *Science*, *325*(5937), 184–187, doi:10.1126/science.1169984.
- Beard, B. L., C. M. Johnson, L. Cox, H. Sun, K. H. Nealson, and C. Aguilar (1999), Iron isotope biosignatures, *Science*, *285*(5435), 1889–1892, doi:10.1126/science.285.5435.1889.
- Beard, B. L., R. M. Handler, M. M. Scherer, L. Wu, A. D. Czaja, A. Heimann, and C. M. Johnson (2010), Iron isotope fractionation between aqueous ferrous iron and goethite, *Earth Planet. Sci. Lett.*, *295*(1–2), 241–250, doi:10.1016/j.epsl.2010.04.006.
- Brantley, S. L., L. J. Liermann, R. L. Guynn, A. Anbar, G. A. Icopini, and J. Barling (2004), Fe isotopic fractionation during mineral dissolution with and without bacteria, *Geochim. Cosmochim. Acta*, *68*(15), 3189–3204, doi:10.1016/j.gca.2004.01.023.
- Br uer, K., H. K mpf, E. Faber, U. Koch, H. M. Nitzsche, and G. Strauch (2005), Seismically triggered microbial methane production relating to the Vogtland—NW Bohemia earthquake swarm period 2000, Central Europe, *Geochem. J.*, *39*(5), 441–450, doi:10.2343/geochemj.39.441.
- Br uer, K., H. K mpf, U. Koch, S. Niedermann, and G. Strauch (2007), Seismically induced changes of the fluid signature detected by a multi-isotope approach (He, CO<sub>2</sub>, CH<sub>4</sub>, N<sub>2</sub>) at the Wetzinquelle, Bad Brambach (central Europe), *J. Geophys. Res.*, *112*, B04307, doi:10.1029/2006JB004404.
- Br uer, K., H. K mpf, S. Niedermann, and G. Strauch (2008), Natural laboratory NW Bohemia: Comprehensive fluid studies between 1992 and 2005 used to trace geodynamic processes, *Geochem. Geophys. Geosyst.*, *9*, Q04018, doi:10.1029/2007GC001921.
- Br uer, K., H. K mpf, U. Koch, and G. Strauch (2011), Monthly monitoring of gas and isotope compositions in the free gas phase at degassing locations close to the Nov y Kostel focal zone in the western Eger Rift, Czech Republic, *Chem. Geol.*, *290*(3–4), 163–176, doi:10.1016/j.chemgeo.2011.09.012.
- Br uer, K., H. K mpf, and G. Strauch (2014), Seismically triggered anomalies in the isotope signatures of mantle-derived gases detected at degassing sites along two neighboring faults in NW Bohemia, central Europe, *J. Geophys. Res. Solid Earth*, *119*, 5613–5632, doi:10.1002/2014jb011044.
- Bullen, T. D., A. F. White, C. W. Childs, D. V. Vivit, and M. S. Schulz (2001), Demonstration of significant abiotic iron isotope fractionation in nature, *Geology*, *29*(8), 699–702, doi:10.1130/0091-7613(2001)029<0699:dosaii>2.0.co;2.
- Chang, Y.-H., T.-W. Cheng, W.-J. Lai, W.-Y. Tsai, C.-H. Sun, L.-H. Lin, and P.-L. Wang (2012), Microbial methane cycling in a terrestrial mud volcano in eastern Taiwan, *Environ. Microbiol.*, *14*(4), 895–908, doi:10.1111/j.1462-2920.2011.02658.x.
- Chao, T. T., and R. F. Sanzolone (1992), Decomposition techniques, *J. Geochem. Explor.*, *44*(1–3), 65–106, doi:10.1016/0375-6742(92)90048-d.
- Chapman, J. B., D. J. Weiss, Y. Shan, and M. Lemburger (2009), Iron isotope fractionation during leaching of granite and basalt by hydrochloric and oxalic acids, *Geochim. Cosmochim. Acta*, *73*(5), 1312–1324, doi:10.1016/j.gca.2008.11.037.
- Coates, J. D., D. J. Ellis, C. V. Gaw, and D. R. Lovley (1999), Geothrix fermentans gen. nov., sp. nov., a novel Fe(III)-reducing bacterium from a hydrocarbon-contaminated aquifer, *Int. J. Syst. Bacteriol.*, *49*, 1615–1622.
- Credner, H. (1876), Das vogtl ndisch-erzgebirgische Erdbeben vom 23. November 1875, *Zeitschrift f r die gesamten Naturwissenschaften*, *48*, 246–269.
- Croal, L. R., C. M. Johnson, B. L. Beard, and D. K. Newman (2004), Iron isotope fractionation by Fe(II)-oxidizing photoautotrophic bacteria, *Geochim. Cosmochim. Acta*, *68*(6), 1227–1242, doi:10.1016/j.gca.2003.09.011.
- Crosby, H. A., E. E. Roden, C. M. Johnson, and B. L. Beard (2007), The mechanisms of iron isotope fractionation produced during dissimilatory Fe(III) reduction by *Shewanella putrefaciens* and *Geobacter sulfurreducens*, *Geobiology*, *5*(2), 169–189, doi:10.1111/j.1472-4669.2007.00103.x.
- Crowe, S. A., et al. (2011), The methane cycle in ferruginous Lake Matano, *Geobiology*, *9*(1), 61–78, doi:10.1111/j.1472-4669.2010.00257.x.
- Dennaud, J., A. Howes, E. Poussel, and J. M. Mermet (2001), Study of ionic-to-atomic line intensity ratios for two axial viewing-based inductively coupled plasma atomic emission spectrometers, *Spectrochim. Acta, Part B*, *56*(1), 101–112, doi:10.1016/s0584-8547(00)00299-8.

- Dulski, P. (2001), Reference materials for geochemical studies: New analytical data by ICP-MS and critical discussion of reference values, *Geostand. Newsl.*, 25(1), 87–125, doi:10.1111/j.1751-908X.2001.tb00790.x.
- Faber, E., J. Horálek, A. Boukova, M. Teschner, U. Koch, and J. Poggenburg (2009), Continuous gas monitoring in the West Bohemian earthquake area, Czech Republic: First results, *Stud. Geophys. Geod.*, 53(3), 315–328, doi:10.1007/s11200-009-0020-z.
- Fischer, T. (2003), The August–December 2000 earthquake swarm in NW Bohemia: The first results based on automatic processing of seismograms, *J. Geodyn.*, 35(1–2), 59–81.
- Fischer, T., and J. Horálek (2005), Slip-generated patterns of swarm microearthquakes from West Bohemia/Vogtland (central Europe): Evidence of their triggering mechanism?, *J. Geophys. Res.*, 110, B05S21, doi:10.1029/2004JB003363.
- Fischer, T., J. Horálek, P. Hrubcova, V. Vavrycuk, K. Bräuer, and H. Kämpf (2014), Intra-continental earthquake swarms in West-Bohemia and Vogtland: A review, *Tectonophysics*, 611, 1–27, doi:10.1016/j.tecto.2013.11.001.
- Förster, H. J. (1998), The chemical composition of REE-Y-Th-U-rich accessory minerals in peraluminous granites of the Erzgebirge-Fichtelgebirge region, Germany. Part II: Xenotime, *Am. Mineral.*, 83(11–12), 1302–1315.
- Förster, H. J. (1999), The chemical composition of uraninite in Variscan granites of the Erzgebirge, Germany, *Mineral. Mag.*, 63(2), 239–252, doi:10.1180/002646199548466.
- Govindaraju, K. (1995), 1995 working values with confidence limits for twenty-six CRPG, ANRT and IWG-GIT geostandards, *Geostand. Newsl.*, 19, 1–32, doi:10.1111/j.1751-908X.1995.tb00164.x.
- Guo, H., C. Liu, H. Lu, R. B. Wanty, J. Wang, and Y. Zhou (2013), Pathways of coupled arsenic and iron cycling in high arsenic groundwater of the Hetao basin, Inner Mongolia, China: An iron isotope approach, *Geochim. Cosmochim. Acta*, 112, 130–145, doi:10.1016/j.gca.2013.02.031.
- Hallbeck, L., F. Stahl, and K. Pedersen (1993), Phylogeny and phenotypic characterization of the stalk-forming and iron-oxidizing bacterium *Gallionella-ferruginea*, *J. Gen. Microbiol.*, 139, 1531–1535.
- Hansen, L. B., K. Finster, H. Fossing, and N. Iversen (1998), Anaerobic methane oxidation in sulfate depleted sediments: Effects of sulfate and molybdate additions, *Aquat. Microb. Ecol.*, 14(2), 195–204, doi:10.3354/ame014195.
- Hecht, L., J. L. Vigneresse, and G. Morteani (1997), Constraints on the origin of zonation of the granite complexes in the Fichtelgebirge (Germany and Czech Republic): Evidence from a gravity and geochemical study, *Geol. Rundsch.*, 86, S93–S109, doi:10.1007/pl00014669.
- Heimann, A., B. Beard, and C. Johnson (2007), Fe isotopes in siliceous igneous rocks: Evidence for fluid-rock interaction in plutons, *Geochim. Cosmochim. Acta*, 71(15), A390–A390.
- Heinicke, J., T. Fischer, R. Gaupp, J. Götz, U. Koch, H. Konietzky, and K. P. Stanek (2009), Hydrothermal alteration as a trigger mechanism for earthquake swarms: The Vogtland/NW Bohemia region as a case study, *Geophys. J. Int.*, 178(1), 1–13, doi:10.1111/j.1365-246X.2009.04138.x.
- Hinrichs, K. U., J. M. Hayes, S. P. Sylva, P. G. Brewer, and E. F. DeLong (1999), Methane-consuming archaeobacteria in marine sediments, *Nature*, 398(6730), 802–805.
- Hoehler, T. M., M. J. Alperin, D. B. Albert, and C. S. Martens (1994), Field and laboratory studies of the methane oxidation in an anoxic marine sediment—Evidence for a methanogen-sulfate reducer consortium, *Global Biogeochem. Cycles*, 8, 451–463, doi:10.1029/94GB01800.
- Horálek, J., and J. Šílený (2013), Source mechanisms of the 2000-earthquake swarm in the West Bohemia/Vogtland region (Central Europe), *Geophys. J. Int.*, 194, 979–999, doi:10.1093/gji/ggt138.
- Horálek, J., and T. Fischer (2008), Role of crustal fluids in triggering the west Bohemian/Vogtland earthquake swarms: Just what we know (a review), *Stud. Geophys. Geod.*, 52(4), 455–478, doi:10.1007/s11200-008-0032-0.
- Horálek, J., and T. Fischer (2010), Intraplate earthquake swarms in West Bohemia/Vogtland (Central Europe), *Jökull*, 60, 67–87.
- Ito, T., K. Nagamine, K. Yamamoto, M. Adachi, and I. Kawabe (1999), Preseismic hydrogen gas anomalies caused by stress-corrosion process preceding earthquakes, *Geophys. Res. Lett.*, 26, 2009–2012, doi:10.1029/1999GL900407.
- Jochum, K. P., L. Nohl, K. Herwig, E. Lammel, B. Stoll, and A. W. Hofmann (2005), GeoReM: A new geochemical database for reference materials and isotopic standards, *Geostand. Geoanal. Res.*, 29(3), 333–338, doi:10.1111/j.1751-908X.2005.tb00904.x.
- Jochum, K. P., U. Weis, B. Schwager, B. Stoll, S. A. Wilson, G. H. Haug, M. O. Andreae, and J. Enzweiler (2016), Reference values following ISO guidelines for frequently requested rock reference materials, *Geostand. Geoanal. Res.*, doi:10.1111/j.1751-908X.2015.00392.x.
- Johnson, C. M., J. L. Skulan, B. L. Beard, H. Sun, K. H. Nealson, and P. S. Braterman (2002), Isotopic fractionation between Fe(III) and Fe(II) in aqueous solutions, *Earth Planet. Sci. Lett.*, 195(1–2), 141–153, doi:10.1016/S0012-821X(01)00581-7.
- Kämpf, H., G. Strauch, P. Vogler, and W. Michler (1989), Hydrologic and hydrochemic changes associated with the December 1985/January 1986 earthquake swarm activity in the Vogtland/NW Bohemia seismic area, *Z. Geol. Wiss.*, 17, 685–698.
- Kämpf, H., K. Bräuer, J. Schumann, K. Hahne, and G. Strauch (2013), CO<sub>2</sub> discharge in an active, non-volcanic continental rift area (Czech Republic): Characterisation (delta C-13, He-3/He-4) and quantification of diffuse and vent CO<sub>2</sub> emissions, *Chem. Geol.*, 339, 71–83, doi:10.1016/j.chemgeo.2012.08.005.
- Kappler, A., C. M. Johnson, H. A. Crosby, B. L. Beard, and D. K. Newman (2010), Evidence for equilibrium iron isotope fractionation by nitrate-reducing iron(II)-oxidizing bacteria, *Geochim. Cosmochim. Acta*, 74(10), 2826–2842, doi:10.1016/j.gca.2010.02.017.
- Kashafi, K., and D. R. Lovley (2003), Extending the upper temperature limit for life, *Science*, 301(5635), 934–934.
- Kietavainen, R., and L. Purkamo (2015), The origin, source, and cycling of methane in deep crystalline rock biosphere, *Front. Microbiol.*, 6, 16, doi:10.3389/fmicb.2015.00725.
- Knett, J. (1899), Das Erzgebirgische Schwarmbeben vom 1. Jänner bis 5. Feber 1824, Sitzungsberichte des Deutschen Naturwissenschaftlich medicinischen Vereins Für Böhmen, LOTOS Prag N.F., 19, 167–191.
- Koch, U., and J. Heinicke (2011), Seismohydrological effects related to the NW Bohemia earthquake swarms of 2000 and 2008: Similarities and distinctions, *J. Geodyn.*, 51(1), 44–52, doi:10.1016/j.jog.2010.07.002.
- Koch, U., J. Heinicke, K. Fröhlich, and M. Krbetschek (1992), Radon im Oberen Vogtland und seine geowissenschaftliche Anwendung, *Wiss. Fortschr.*, 42, 253–255.
- Koch, U., D. Hebert, M. Voßberg, and J. Heinicke (2005), Auswirkungen der Fassungssanierung der Wetzinquelle, Bad Brambach, auf die Altersstruktur des Mineralwassers, *Grundwasser*, 10(2), 102–113, doi:10.1007/s00767-005-0081-z.
- Koch, U., K. Bräuer, J. Heinicke, and H. Kämpf (2008), The gas flow at mineral springs and mofettes in the Vogtland/NW Bohemia: An enduring long-term increase, *Geofluids*, 8(4), 274–285, doi:10.1111/j.1468-8123.2008.00230.x.
- Kodama, Y., and K. Watanabe (2004), Sulfuricurvum kujiense gen. nov., sp nov., a facultatively anaerobic, chemolithoautotrophic, sulfur-oxidizing bacterium isolated from an underground crude-oil storage cavity, *Int. J. Syst. Evol. Microbiol.*, 54, 2297–2300, doi:10.1099/ijs.0.63243-0.
- Li, J. (1996), Improving analytical precision by utilizing intrinsic internal standards for determining minor constituents by inductively coupled plasma atomic emission spectrometry, *J. Anal. Atom. Spectrom.*, 11(9), 683–687, doi:10.1039/ja9961100683.
- Lin, L.-H., et al. (2006), Long-term sustainability of a high-energy, low-diversity crustal biome, *Science*, 314(5798), 479–482, doi:10.1126/science.1127376.

- Marcos, A., M. Foulkes, and S. J. Hill (2001), Application of a multi-way method to study long-term stability in ICP-AES, *J. Anal. Atom. Spectrom.*, *16*(2), 105–114, doi:10.1039/b008759i.
- Markl, G., F. von Blanckenburg, T. Wagner, and I. Horn (2007), Iron isotope fractionation during hydrothermal ore deposition and alteration, *Geochim. Cosmochim. Acta*, *71*(15), A622–A622.
- Mikutta, C., J. G. Wiederhold, O. A. Cirpka, T. B. Hofstetter, B. Bourdon, and U. Von Gunten (2009), Iron isotope fractionation and atom exchange during sorption of ferrous iron to mineral surfaces, *Geochim. Cosmochim. Acta*, *73*(7), 1795–1812, doi:10.1016/j.gca.2009.01.014.
- Moeller, K., R. Schoenberg, T. Grenne, I. H. Thorseth, K. Drost, and R. B. Pedersen (2014), Comparison of iron isotope variations in modern and Ordovician siliceous Fe oxyhydroxide deposits, *Geochim. Cosmochim. Acta*, *126*, 422–440.
- Morgan, J. L. L., L. E. Wasylenki, J. Nuester, and A. D. Anbar (2010), Fe isotope fractionation during equilibration of Fe-Organic complexes, *Environ. Sci. Technol.*, *44*(16), 6095–6101, doi:10.1021/es100906z.
- Mrlina, J., H. Kämpf, C. Kroner, J. Mingram, M. Stebich, A. Brauer, W. H. Geissler, J. Kallmeyer, H. Matthes, and M. Seidl (2009), Discovery of the first Quaternary maar in the Bohemian Massif, central Europe, based on combined geophysical and geological surveys, *J. Volcanol. Geotherm. Res.*, *182*(1–2), 97–112, doi:10.1016/j.jvolgeores.2009.01.027.
- Mulholland, D. S., F. Poitrasson, L. S. Shirokova, A. G. Gonzalez, O. S. Pokrovsky, G. R. Boaventura, and L. C. Vieira (2015), Iron isotope fractionation during Fe(II) and Fe(III) adsorption on cyanobacteria, *Chem. Geol.*, *400*, 24–33, doi:10.1016/j.chemgeo.2015.01.017.
- Neunhöfer, H., and A. Hemmann (2005), Earthquake swarms in the Vogtland/Western Bohemia region: Spatial distribution and magnitude-frequency distribution as an indication of the genesis of swarms?, *J. Geodyn.*, *39*(4), 361–385, doi:10.1016/j.jog.2005.01.004.
- Nickschick, T., H. Kämpf, C. Flechsig, J. Mrlina, and J. Heinicke (2015), CO<sub>2</sub> degassing in the Hartouov mofette area, western Eger Rift, imaged by CO<sub>2</sub> mapping and geoelectrical and gravity surveys, *Int. J. Earth Sci.*, *104*(8), 2107–2129, doi:10.1007/s00531-014-1140-4.
- Pedersen, K. (2000), Exploration of deep intraterrestrial microbial life: Current perspectives, *Fems Microbiol. Lett.*, *185*(1), 9–16, doi:10.1016/s0378-1097(00)00061-6.
- Pedersen, K. (2012), Subterranean microbial populations metabolize hydrogen and acetate under in situ conditions in granitic groundwater at 450 m depth in the Aspo Hard Rock Laboratory, Sweden, *Fems Microbiol. Ecol.*, *81*(1), 217–229, doi:10.1111/j.1574-6941.2012.01370.x.
- Peterek, A., C.-D. Reuther, and R. Schunk (2011), Neotectonic evolution of the Cheb Basin (Northwestern Bohemia, Czech Republic) and its implications for the late Pliocene to Recent crustal deformation in the western part of the Eger Rift, *Z. Geol. Wiss.*, *39*(5/6), 335–365.
- Poitrasson, F., and R. Freyrier (2005), Heavy iron isotope composition of granites determined by high resolution MC-ICP-MS, *Chem. Geol.*, *222*(1–2), 132–147, doi:10.1016/j.chemgeo.2005.07.005.
- Poitrasson, F., S. H. Dundas, J. P. Toutain, M. Munoz, and A. Rigo (1999), Earthquake-related elemental and isotopic lead anomaly in a springwater, *Earth Planet. Sci. Lett.*, *169*(3–4), 269–276, doi:10.1016/s0012-821x(99)00085-0.
- Polyakov, V. B., and S. D. Mineev (2000), The use of Mossbauer spectroscopy in stable isotope geochemistry, *Geochim. Cosmochim. Acta*, *64*(5), 849–865, doi:10.1016/s0016-7037(99)00329-4.
- Potts, P. J. (1987), *A Handbook of Silicate Rock Analysis*, pp. 622, Blackie, Glasgow.
- Reddy, D. V., P. Nagabhushanam, and B. S. Sukhija (2011), Earthquake (M 5.1) induced hydrogeochemical and delta O-18 changes: Validation of aquifer breaching-mixing model in Koyna, India, *Geophys. J. Int.*, *184*(1), 359–370, doi:10.1111/j.1365-246X.2010.04838.x.
- Riley, J. P. (1958), The rapid analysis of silicate rocks and minerals, *Anal. Chim. Acta*, *19*, 413–428, doi:10.1016/S0003-2670(00)88187-8.
- Robertson, L. A., and J. G. Kuenen (2006), *The Prokaryotes: Volume 5: Proteobacteria: Alpha and Beta Subclasses*, Springer, New York.
- Saunier, G., G. S. Pokrovski, and F. Poitrasson (2011), First experimental determination of iron isotope fractionation between hematite and aqueous solution at hydrothermal conditions, *Geochim. Cosmochim. Acta*, *75*(21), 6629–6654, doi:10.1016/j.gca.2011.08.028.
- Schoenberg, R., and F. von Blanckenburg (2005), An assessment of the accuracy of stable Fe isotope ratio measurements on samples with organic and inorganic matrices by high-resolution multicollector ICP-MS, *Int. J. Mass Spectrom.*, *242*(2–3), 257–272, doi:10.1016/j.jjms.2004.11.025.
- Schreiber, U., O. Locker-Gruetjen, and C. Mayer (2012), Hypothesis: Origin of life in deep-reaching tectonic faults, *Origins Life Evol. Biospheres*, *42*(1), 47–54, doi:10.1007/s11084-012-9267-4.
- Schuth, S., J. Hurrass, C. Muenker, and T. Mansfeldt (2015), Redox-dependent fractionation of iron isotopes in suspensions of a groundwater-influenced soil, *Chem. Geol.*, *392*, 74–86, doi:10.1016/j.chemgeo.2014.11.007.
- Sherwood Lollar, B., K. Voglesonger, L. H. Lin, G. Lacrampe-Couloume, J. Telling, T. A. Abrajano, T. C. Onstott, and L. M. Pratt (2007), Hydrogeologic controls on episodic H-2 release from Precambrian fractured rocks—Energy for deep subsurface life on Earth and Mars, *Astrobiology*, *7*(6), 971–986, doi:10.1089/ast.2006.0096.
- Sherwood Lollar, B., T. C. Onstott, G. Lacrampe-Couloume, and C. J. Ballentine (2014), The contribution of the Precambrian continental lithosphere to global H-2 production, *Nature*, *516*(7531), 379–382, doi:10.1038/nature14017.
- Sivan, O., M. Adler, A. Pearson, F. Gelman, I. Bar-Or, S. G. John, and W. Eckert (2011), Geochemical evidence for iron-mediated anaerobic oxidation of methane, *Limnol. Oceanogr.*, *56*(4), 1536–1544, doi:10.4319/lo.2011.56.4.1536.
- Sivan, O., S. S. Shusta, and D. L. Valentine (2016), Methanogens rapidly transition from methane production to iron reduction, *Geobiology*, *14*(2), 190–203, doi:10.1111/gbi.12172.
- Skelton, A., et al. (2014), Changes in groundwater chemistry before two consecutive earthquakes in Iceland, *Nat. Geosci.*, *7*(10), 752–756, doi:10.1038/ngeo2250.
- Skulan, J. L., B. L. Beard, and C. M. Johnson (2002), Kinetic and equilibrium Fe isotope fractionation between aqueous Fe(III) and hematite, *Geochim. Cosmochim. Acta*, *66*(17), 2995–3015, doi:10.1016/s0016-7037(02)00902-x.
- Taran, Y. A., A. Ramirez-Guzman, R. Bernard, E. Cienfuegos, and P. Morales (2005), Seismic-related variations in the chemical and isotopic composition of thermal springs near Acapulco, Guerrero, Mexico, *Geophys. Res. Lett.*, *32*, L14317, doi:10.1029/2005GL022726.
- Teutsch, N., U. von Gunten, D. Porcelli, O. A. Cirpka, and A. N. Halliday (2005), Adsorption as a cause for iron isotope fractionation in reduced groundwater, *Geochim. Cosmochim. Acta*, *69*(17), 4175–4185, doi:10.1016/j.gca.2005.04.007.
- Totland, M., I. Jarvis, and K. E. Jarvis (1992), An assessment of dissolution techniques for the analysis of geological samples by plasma spectrometry, *Chem. Geol.*, *95*(1–2), 35–62, doi:10.1016/0009-2541(92)90042-4.
- Toutain, J. P., M. Munoz, J. L. Pinaud, S. Levet, M. Sylvander, A. Rigo, and J. Escalier (2006), Modelling the mixing function to constrain coseismic hydrochemical effects: An example from the French Pyrenees, *Pure Appl. Geophys.*, *163*(4), 723–744, doi:10.1007/s00024-006-0047-9.
- Tsunogai, U., and H. Wakita (1995), Precursory chemical-changes in-ground water—Kobe earthquake, Japan, *Science*, *269*(5220), 61–63.
- Vyllita, T., K. Zak, V. Cilex, H. Hercman, and L. Miksikova (2007), Evolution of hot-spring travertine accumulation in Karlovy Vary/Carlsbad (Czech Republic) and its significance for the evolution of Tepla valley and Ohre/Eger rift, *Z. Geomorphol.*, *51*(4), 427–442, doi:10.1127/0372-8854/2007/0051-0427.
- Wagner, C., M. Mau, M. Schloemann, J. Heinicke, and U. Koch (2007), Characterization of the bacterial flora in mineral waters in upstreaming fluids of deep igneous rock aquifers, *J. Geophys. Res.*, *112*, G01003, doi:10.1029/2005JG000105.

- Walsh, J. N. (1992), Use of multiple internal standards for high-precision, routine analysis of geological samples by inductively coupled plasma atomic emission spectrometry, *Chem. Geol.*, *95*(1–2), 113–121, doi:10.1016/0009-2541(92)90048-a.
- Wasteby, N., A. Skelton, E. Tollefsen, M. Andren, G. Stockmann, L. C. Liljedahl, E. Sturkell, and M. Morth (2014), Hydrochemical monitoring, petrological observation, and geochemical modeling of fault healing after an earthquake, *J. Geophys. Res. Solid Earth*, *119*, 5727–5740, doi:10.1002/2013jb010715.
- Watznauer, A., and U. Koch (1989), Die geologischen und hydrologischen Verhältnisse im Quellgebiet von Bad Brambach, *Abh. SAW Leipzig Math. Nat. Klasse*, *57*, 49–58.
- Weinlich, F. H., K. Bräuer, H. Kämpf, G. Strauch, J. Tesar, and S. M. Weise (1999), An active subcontinental mantle volatile system in the western Eger rift, central Europe: Gas flux, isotopic (He, C, and N) and compositional fingerprints, *Geochim. Cosmochim. Acta*, *63*(21), 3653–3671, doi:10.1016/s0016-7037(99)00187-8.
- Weise, S. M., K. Bräuer, H. Kämpf, G. Strauch, and U. Koch (2001), Transport of mantle volatiles through the crust traced by seismically released fluids: A natural experiment in the earthquake swarm area Vogtland/NW Bohemia, central Europe, *Tectonophysics*, *336*(1–4), 137–150, doi:10.1016/s0040-1951(01)00098-1.
- Welch, S. A., B. L. Beard, C. M. Johnson, and P. S. Braterman (2003), Kinetic and equilibrium Fe isotope fractionation between aqueous Fe(II) and Fe(III), *Geochim. Cosmochim. Acta*, *67*(22), 4231–4250, doi:10.1016/s0016-7037(03)00266-7.
- Wiederhold, J. G. (2015), Metal stable isotope signatures as tracers in environmental geochemistry, *Environ. Sci. Technol.*, *49*(5), 2606–2624, doi:10.1021/es504683e.
- Wiesli, R. A., B. L. Beard, and C. M. Johnson (2004), Experimental determination of Fe isotope fractionation between aqueous Fe(II), siderite and “green rust” in abiotic systems, *Chem. Geol.*, *211*(3–4), 343–362, doi:10.1016/j.chemgeo.2004.07.002.
- Woith, H., R. J. Wang, U. Maiwald, A. Pekdeger, and J. Zschau (2013), On the origin of geochemical anomalies in groundwaters induced by the Adana 1998 earthquake, *Chem. Geol.*, *339*, 177–186, doi:10.1016/j.chemgeo.2012.10.012.
- Xie, X. J., T. M. Johnson, Y. X. Wang, C. C. Lundstrom, A. Ellis, X. L. Wang, M. Y. Duan, and J. X. Li (2014), Pathways of arsenic from sediments to groundwater in the hyporheic zone: Evidence from an iron isotope study, *J. Hydrol.*, *511*, 509–517, doi:10.1016/j.jhydrol.2014.02.006.
- Yeghicheyan, D., et al. (2013), A compilation of silicon, rare earth element and twenty-one other trace element concentrations in the natural river water reference material SLRS-5 (NRC-CNRC), *Geostand. Geoanal. Res.*, *37*(4), 449–467, doi:10.1111/j.1751-908X.2013.00232.x.